Journal of Experimental Botany, Vol. 64, No. 12, pp. 3583–3604, 2013
doi:10.1093/jxb/ert191 Advance Access publication 23 July, 2013
This paper is available online free of all access charges (see http://jxb.oxfordjournals.org/open_access.html for further details)

Journal of Experimental Botany
www.jxb.oxfordjournals.org

RESEARCH PAPER

Structural and physiological analyses in Salsoleae (Chenopodiaceae) indicate multiple transitions among C_3, intermediate, and C_4 photosynthesis

Elena V. Voznesenskaya[1], Nuria K. Koteyeva[1], Hossein Akhani[2,*], Eric H. Roalson[3] and Gerald E. Edwards[3,*]

[1] Laboratory of Anatomy and Morphology, V. L. Komarov Botanical Institute of Russian Academy of Sciences, Prof. Popov Street 2, 197376 Saint Petersburg, Russia

[2] Department of Plant Sciences, School of Biology and Center of excellence in Phylogeny of Living Organisms, College of Sciences, University of Tehran, PO Box 14155-6455, Tehran, Iran

[3] School of Biological Sciences, Washington State University, Pullman, WA 99164-4236, USA

* To whom correspondence should be addressed. E-mail: edwardsg@wsu.edu *or* akhani@khayam.ut.ac.ir

Received 21 February 2013; Revised 24 May 2013; Accepted 28 May 2013

Abstract

In subfamily Salsoloideae (family Chenopodiaceae) most species are C_4 plants having terete leaves with Salsoloid Kranz anatomy characterized by a continuous dual chlorenchyma layer of Kranz cells (KCs) and mesophyll (M) cells, surrounding water storage and vascular tissue. From section *Coccosalsola sensu* Botschantzev, leaf structural and photosynthetic features were analysed on selected species of *Salsola* which are not performing C_4 based on leaf carbon isotope composition. The results infer the following progression in distinct functional and structural forms from C_3 to intermediate to C_4 photosynthesis with increased leaf succulence without changes in vein density: From species performing C_3 photosynthesis with Sympegmoid anatomy with two equivalent layers of elongated M cells, with few organelles in a discontinuous layer of bundle sheath (BS) cells (*S. genistoides*, *S. masenderanica*, *S. webbii*) > development of proto-Kranz BS cells having mitochondria in a centripetal position and increased chloroplast number (*S. montana*) > functional C_3–C_4 intermediates having intermediate CO_2 compensation points with refixation of photorespired CO_2, development of Kranz-like anatomy with reduction in the outer M cell layer to hypodermal-like cells, and increased specialization (but not size) of a Kranz-like inner layer of cells with increased cell wall thickness, organelle number, and selective expression of mitochondrial glycine decarboxylase (Kranz-like Sympegmoid, *S. arbusculiformis*; and Kranz-like Salsoloid, *S. divaricata*) > selective expression of enzymes between the two cell types for performing C_4 with Salsoloid-type anatomy. Phylogenetic analysis of tribe Salsoleae shows the occurrence of C_3 and intermediates in several clades, and lineages of interest for studying different forms of anatomy.

Key words: C_3 plants, C_3–C_4 intermediate, C_4 plants, Chenopodiaceae, immunolocalization, leaf anatomy, photosynthetic enzymes, *Salsola divaricata*, *Salsola genistoides*, *Salsola masenderanica*, *Salsola montana*, *Salsola webbii*.

Introduction

Among eudicot families, it is well established that family Chenopodiaceae has the largest number of C_4 species (Akhani et al., 1997; Kadereit and Freitag, 2011; Sage et al., 2012), and also the greatest diversity in C_4-type leaf anatomy, with eight main structural types (Carolin et al., 1975; Edwards and Voznesenskaya, 2011), and up to 16 forms considering all

Abbreviations: BS, bundle sheath; Γ, CO_2 compensation point; GDC, glycine decarboxylase; IS, intercellular air space; KC, Kranz cell; KLC, Kranz-like cell; M, mesophyll; NAD-ME, NAD-malic enzyme; NADP-ME, NADP-malic enzyme; PEPC, phosphoenolpyruvate carboxylase; PEP-CK, phosphoenolpyruvate carboxykinase; Rubisco, ribulose 1,5-bisphosphate carboxylase-oxygenase; WS, water storage.

differences (Kadereit et al., 2003). This includes the occurrence of Kranz anatomy around individual veins as well as Kranz anatomy with a concentric dual layer of cells surrounding all the veins in the leaf, and two structural forms of C_4 occurring in individual cells without Kranz anatomy. Currently, 10 C_4 lineages have been recognized in Chenopodiaceae (Kadereit and Freitag, 2011; Sage et al., 2012).

C_3–C_4 intermediates are important in studying the evolution of C_4 photosynthesis. They have been identified in 14 families: Amaranthaceae, Asteraceae, Boraginaceae, Brassicaceae, Chenopodiaceae, Cleomaceae, Euphorbiaceae, Molluginaceae, Nyctaginaceae, Portulacaceae, Cyperaceae, Hydrocharitaceae, Scrophulariaceae, and Poaceae (Sage et al., 2011; Khoshravesh et al., 2012). However, despite the diversity of C_4 in family Chenopodiaceae, to date only one species, *Salsola arbusculiformis* in subfamily Salsoloideae, has been structurally and functionally characterized to be a C_3–C_4 intermediate (Voznesenskaya et al., 2001). Another species, *Sedobassia sedoides* in subfamily Camphorosmoideae, was recently suggested to be an intermediate based on anatomical features (Kadereit and Freitag, 2011); and shown to function as an intermediate based on gas exchange analysis and immunolocalization of glycine decarboxylase (GDC) (NKK, EVV, and GEE, unpublished data).

In Chenopodiaceae, most species which have been analysed in subfamily Salsoloideae have C_4-type photosynthesis and Kranz anatomy (Zalenskii and Glagoleva, 1981; Pyankov and Vakhrusheva, 1989; Pyankov et al., 1999, 2000, 2001*a*, 2002). Most representatives of the genus *Salsola* sensu lato (s.l.) are C_4 plants with the so-called Salsoloid (Carolin et al., 1975) or 'crown-centric' (Voznesenskaya and Gamaley, 1986; Edwards and Voznesenskaya, 2011) type of Kranz leaf anatomy with two layers of chlorenchyma on the leaf periphery. The outer layer of chlorenchyma is represented by elongated palisade mesophyll (M) cells and the inner layer consists of roundish specialized Kranz cells (KCs). The main vascular bundle is in the centre of the leaf surrounded by the water storage (WS) tissue, and only small, peripheral bundles have contact with chlorenchyma. In this anatomical type, peripheral bundles have their xylem part facing towards the outer chlorenchyma layers (see Edwards and Voznesenskaya, 2011). Also, there are two groups of species in tribe Salsoleae and within the genus *Salsola* s.l., one group lacking and the other group having hypodermal tissue (a subepidermal layer of roundish parenchyma cells which participates in water storage and has a lower number of organelles compared with M cells). C_4 species from sections *Caroxylon* and *Coccosalsola* have a hypoderm, but the hypoderm is absent in species from sections *Malpighipila*, *Cardiandra*, *Belanthera*, and *Salsola* (Pyankov et al., 2001*a*). Molecular phylogenetic analyses suggest that the traditionally recognized sections of *Salsola* are not monophyletic; a revised, clade-based classification has recently reorganized sectional and generic boundaries (Akhani et al., 2007).

Studies on C_4 photosynthesis have been largely focused on species which form Kranz anatomy with two chlorenchyma layers surrounding each vein (called a multiple simple Kranz unit by Peter and Katinas, 2003), as occurs in C_4 monocots and numerous C_4 eudicot species. However, among C_4 eudicots, there are nine types of Kranz anatomy with two concentric chlorenchyma layers surrounding all veins (single compound Kranz unit according to Peter and Katinas, 2003); see Edwards and Voznesenskaya (2011). Among these is the Salsoloid type of anatomy which is characteristic for C_4 species in subfamily Salsoloideae. Current, commonly used structural descriptions of the dual layer of cells forming Kranz anatomy refer to the outer layer as M cells (usually consisting of palisade parenchyma) and the inner layer as specialized bundle sheath (BS) cells (referring to a layer of cells in leaves of plants which surrounds the vascular tissue). However, in C_4 species such as the Salsoloid type, the inner chlorenchyma layer does not form a real sheath around individual peripheral veins, but rather a sheath which encloses the veins and WS tissue. Thus, here the inner layer of chlorenchyma cells which are specialized for C_4 photosynthesis is referred to as the KC layer (Edwards and Voznesenskaya, 2011). All structural forms of Kranz have in common a double concentric layer of chlorenchyma cells with the outer layer of palisade M capturing atmospheric CO_2 in the C_4 cycle, and the inner layer (BS cells or KCs) donating CO_2 from C_4 acids to Rubisco in the C_3 cycle.

It is also known that some species in genus *Salsola* s.l. have a different type of leaf anatomy, with multiple layers of chlorenchyma and, adjacent to veins, indistinctive BS cells with few chloroplasts. This type, described by Carolin et al. (1975) in *Salsola webbii* and in the genus *Sympegma*, was designated 'Sympegmoid', and defined as having non-Kranz-type anatomy. Analysis of the carbon isotope composition ($\delta^{13}C$) of plant biomass showed that *S. webbii* has C_3-type values (Akhani et al., 1997; Winter, 1981). To date, several species in the genus *Salsola* have been identified as having this C_3-like leaf anatomy and/or C_3-type $\delta^{13}C$: namely, *S. abrotanoides* (Pyankov et al., 2001*b*), *S. botschantzevii* (Pyankov et al., 2001*b*), *S. divaricata* (Pyankov et al., 2001*b*), *S. genistoides* (Voznesenskaya, 1976; Akhani et al., 1997; Pyankov et al., 2001*b*), *S. drobovii* (Butnik, 1984; Pyankov et al., 2001*b*), *S. laricifolia* (Wen and Zhang, 2011), *S. masenderanica* (Pyankov et al., 2001*b*), *S. montana* (Akhani et al., 1997; Akhani and Ghasemkhani, 2007), *S. oreophila* (Pyankov et al., 1997), *S. pachyphylla* (Butnik, 1984), *S. tianshanica* (Pyankov et al., 2001*b*), and *S. webbii* (Carolin et al., 1975; Winter, 1981; Akhani et al., 1997; Pyankov et al., 2001*b*). *Salsola arbusculiformis* has C_3-type carbon isotope composition (Akhani et al., 1997; Akhani and Ghasemkhani, 2007) and intermediate anatomy with Kranz-like BS cells around the veins (Pyankov et al., 1997; Voznesenskaya et al., 2001). According to Botschantzev (1969, 1976, 1985, 1989), all of them belong to section *Coccosalsola* in genus *Salsola* and were classified in the following subsections: *Genistoides* (*S. abrotanoides*, *S. genistoides*, and *S. webbii*), *Coccosalsola* (*S. divaricata*), and *Arbusculae* (other species). Akhani et al. (2007) showed that section *Coccosalsola* is polyphyletic and rearranged the species of this group in the clade-based genera.

Further examination of the inter-relationships between structure and biochemistry in *Salsola* species having Sympegmoid leaf structure showed that *S. oreophila*, a close

relative of *S. montana*, has C_3-type $\delta^{13}C$ values and low activity of C_4 enzymes (Pyankov et al., 1997). It also has 2–3 layers of M and thin-walled BS cells with sparse chloroplasts distributed usually in the centrifugal position; thus, all structural features in this species are C_3 like. In contrast, *S. arbusculiformis* was suggested to be a C_3–C_4 intermediate. Although it usually has two layers of M cells, its BS was found to be Kranz like, containing rather numerous chloroplasts in the centripetal position, and the walls of these cells were thicker than in the M (Pyankov et al., 1997). A detailed study of the anatomy, biochemistry, and physiology of this species showed that it is a C_3–C_4 intermediate (Voznesenskaya et al., 2001). It has an intermediate-type photosynthetic CO_2 response curve with a CO_2 compensation point (Γ) midway between characteristic of C_3 and C_4 species. Photorespiration was shown to be reduced by exclusive localization of GDC to BS mitochondria (a diagnostic feature of all intermediates and C_4 plants) which allows the photorespired CO_2 to be partially refixed. It is classified as a type I intermediate as it lacks a partially functional C_4 cycle (see Edwards and Ku, 1987).

In the present study, the carbon isotope composition was analysed for all species of polyphyletic section *Coccosalsola* (recorded by Botschantzev, 1976, 1989), including *S. botschantzevii* (Botschantzev et al., 1983) and *S. drummondii* (Freitag and Rilke, 1997), of which a large number have C_3-type values (approximately half of the 36 species). A comprehensive anatomical and physiological characterization was performed for five *Salsola* species in the section having C_3-type $\delta^{13}C$ values: *S. divaricata*, *S. genistoides*, *S. masenderanica*, *S. montana*, and *S. webbii*, and the results were analysed relative to two C_4 species, *Caroxylon orientale* (= *Salsola orientalis*) and *Xylosalsola richteri* (= *S. richteri*). The results show that section *Coccosalsola*, which does not form a monophyletic group relative to other sections of *Salsola* and other genera of the Salsoleae (Akhani et al., 2007), has large diversity in forms of photosynthesis. Species in tribe Salsoleae are of interest for studying the evolution of a form of C_4 anatomy where a single, continuous layer of Kranz tissue surrounds the veins and WS cells, as opposed to the occurrence of Kranz anatomy around individual veins. Differences in structural and functional traits were identified which suggest how Salsoloid-type C_4 photosynthesis evolved from C_3 ancestors.

Materials and methods

Plant material

Seeds of *S. divaricata* Masson ex Link were collected in the Canary Islands (Canaria, western coasts, near Agaete, 23.9.2002, H. Akhani 16469), while seeds of *S. masenderanica* Botsch. were collected from N Iran (Mazandaran, 169 km to Tehran, 5 km after Veresk towards Amol, 1201 m, 16.10.2003, H. Akhani 17403) and seeds of *S. montana* Litv. were collected from NE Iran (Golestan, southern parts of Golestan National Park, near Sharlegh, 15.10.2003, H. Akhani 17391). Voucher specimens are available in the Halophytes and C_4 Plants Research Laboratory, School of Biology, University of Tehran (Hb. Akhani). Seeds of *S. webbii* Moq. and *S. genistoides* Juss. ex Poir. were provided via Jeroni Galmes from the Germplasm Collection of the University of Almería (GERMHUAL), research group RNM-344, and Forestaria S.L (see Supplementary Appendix S1 available at *JXB* online for GenBank accession numbers for new sequence information on these two species and voucher numbers of specimens in the WSU Herbarium). Seeds of *Xylosalsola richteri* (Moq.) Akhani & E. H. Roalson (=*Salsola richteri* Moq.) and *Caroxylon orientale* (S.G. Gmel.) Tzvelev (=*Salsola orientalis* S.G. Gmel.) were collected in deserts of Central Asia in Uzbekistan. Seeds were stored at –18 ºC before germination. They were germinated on moist paper at room temperature and then transplanted to soil. For studies on light and electron microscopy, polysaccharide content, enzyme content, and gas exchange, all plants were grown under the same conditions (in Enconair Ecological chambers, model GC-16) under a photosynthetic photon flux density (PPFD) of ~400 µmol quanta m^{-2} s^{-1} with a 14 h/10 h light/dark photoperiod and 25/18 ºC day/night temperature regime. Figure 1 shows the appearance of the plants during growth in the WSU chambers (Fig. 1A, D, G, J, M) and their branches (Fig. 1B, E, H, K, N), and the fruiting branches of the plants grown in nature (Fig. 1C, F, I, L, O). All species have terete succulent leaves. In *S. masenderanica*, *S. montana*, *S. webbii*, and *S. divaricata*, young plants and vegetative branches have rather long leaves (up to 2–2.5 cm) (Fig. 1E, H, N) compared with shorter leaves (up to 1 cm) in growth chamber-grown plants of *S. genistoides* beginning from the early stages of seedling growth (Fig. 1A, B). Leaves were sampled from plants of different ages, from 6 week up to 2 years old. Samples of fully expanded leaves were taken from recently developed vegetative branches at the same time for determination of enzyme content and for light and electron microscopy. For most species, samples were taken from at least two or three individual plants. For comparison, two C_4 *Salsola* s.l. species, which represent two biochemical subtypes in Salsoloideae, were analysed, *X. richteri*, an NADP-malic enzyme (NADP-ME) species, and *C. orientale*, an NAD-ME species.

Light and electron microscopy

Samples for ultrastructural characterization were fixed overnight at 4 °C in 2% (v/v) paraformaldehyde and 2 % (v/v) glutaraldehyde in 0.1 M phosphate buffer (pH 7.2), post-fixed in 2% (w/v) OsO_4, and then, after a standard acetone dehydration procedure, embedded in Spurr's resin. Cross-sections were made on a Reichert Ultracut R ultramicrotome (Reichert-Jung GmbH, Heidelberg, Germany). For light microscopy, semi-thin sections were stained with 1% (w/v) Toluidine blue O in 1% (w/v) $Na_2B_4O_7$, and studied under an Olympus BH-2 (Olympus Optical Co., Ltd) light microscope equipped with an LM Digital Camera and Software (Jenoptik ProgRes Camera, C12plus, Jena, Germany). Ultra-thin sections were stained for electron microscopy with 2% (w/v) uranyl acetate followed by 2% (w/v) lead citrate. Hitachi H-600 (Hitachi Scientific Instruments, Tokyo, Japan), JEOL JEM-1200 EX (JEOL USA, Inc., MA, USA) with MegaView III Camera and Soft Imaging System Corp. (Lakewood, CO, USA) and FEI Tecnai G2 (Field Emission Instruments Company, Hillsboro, OR, USA) equipped with Eagle FP 5271/82 4K HR200KV digital camera transmission electron microscopes were used for observation and photography.

For quantitative characterization of leaf tissues, cells, and organelles, the image analysis program ImageJ 1.37v (Wayne Rasband, National Institutes of Health, USA) was used. The sizes of the cells and areas of the tissues in the leaves were measured on light microscopy images of leaf cross-sections. The volume density of each tissue of interest was estimated from the ratio of the area of the tissue to the total leaf area (expressed as a percentage). The thickness of cell walls (CWs) and the size of mitochondria were measured on electron microscopy images from leaf cross-sections. The small diameters of mitochondria were measured on profiles from cross-sections. As was previously noted in quantitative studies, only the small diameter reflects the difference in size between different tissues or species since measurements of elongation are more variable as very elongated mitochondria are occasionally observed in microscopy sections (see Voznesenskaya et al., 2007). For all measurements, 15–25 micrographs were used for analysis from at least 2–3 different leaves.

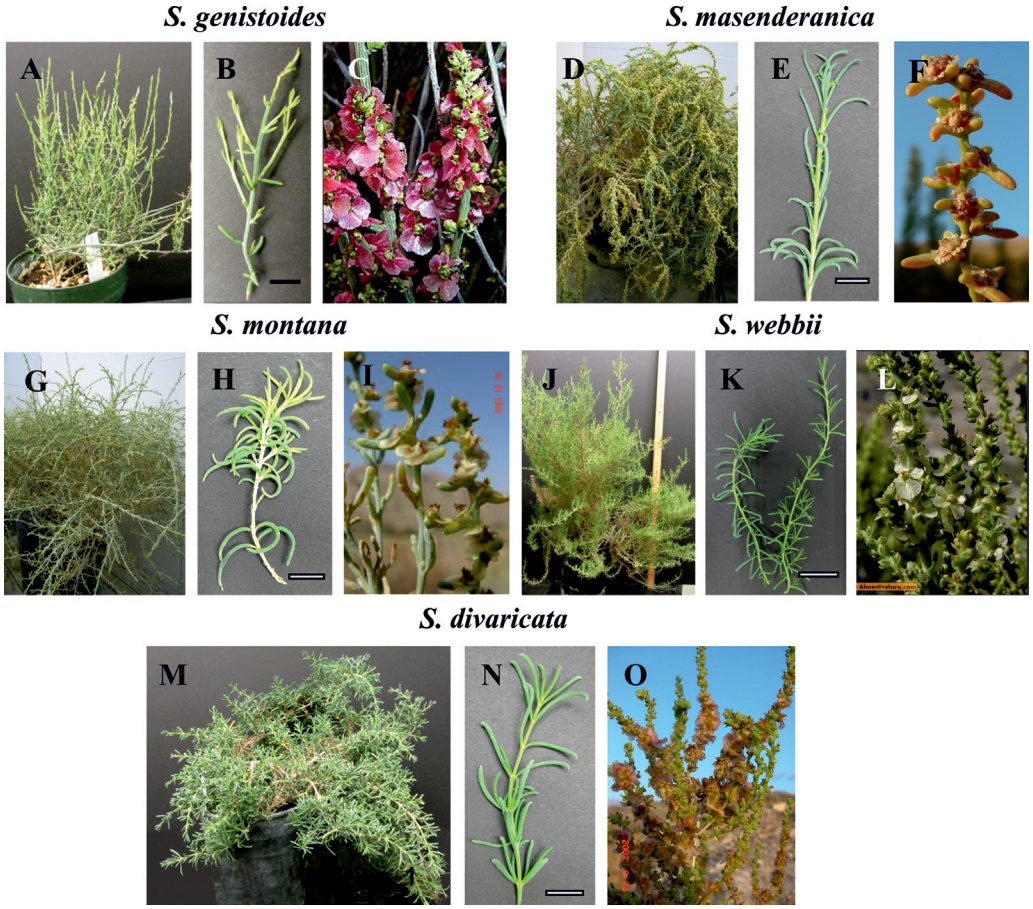

Fig. 1. General views of growth chamber-grown plants (A, D, G, J, M) and their branches (B, E, H, K, N), and the fruiting branches from natural habitats (C, F, I, L, O) of five Salsoleae species formerly classified under *Salsola* section *Coccosalsola*. *Salsola genistoides* (A–C), *S. masenderanica* (D–F), *S. montana* (G–I), *S. webbii* (J–L), and *S. divaricata* (M–O). C, from Herbario virtual de la Universidad de Alicante: http://www.herbariovirtual.ua.es/hoja_salsola_genistoides.htm with permission, accessed 2 April 2013; F, I, O, by HA; L, from AlmeriNatura: http://www.almerinatura.com/, accessed 2 April 2013 with permission. Scale bars=1 cm.

To observe the pattern of leaf venation, leaves were cleared in 70% ethanol (v/v) until chlorophyll was removed, bleached with 5% (w/v) NaOH overnight, and then rinsed three times in water. At least three leaves from two different plants were used. The pattern and density (per mm^2 of the leaf surface area) of the peripheral venation were determined using hand-made paradermal sections. The leaf samples were mounted in water and examined under UV light [with a 4′,6-diamidino-2-phenylindole (DAPI) filter] on a Leica DMFSA fluorescence microscope (Leica Microsystems Wetzlar GmbH, Germany).

In situ *immunolocalization*

Leaf samples were fixed at 4 °C in 2% (v/v) paraformaldehyde and 1.25% (v/v) glutaraldehyde in 0.05 M PIPES buffer, pH 7.2 early in the morning. The samples were dehydrated with a graded ethanol series and embedded in London Resin White (LR White, Electron Microscopy Sciences, Fort Washington, PA, USA) acrylic resin. The antibody used (raised in rabbit) was against the P subunit of GDC from *Pisum sativum* L. (courtesy of D. Oliver). Pre-immune serum was used for controls.

For transmission electron microscopy (TEM) immunolabelling, thin sections on formvar-coated nickel grids were incubated for 1 h in TRIS-buffered saline–Tween (TBST)+bovine serum albumin (BSA) to block non-specific protein binding on the sections. They were then incubated for 3 h with either the pre-immune serum diluted in TBST+BSA (1:50) or anti-P protein of GDC (1:10) antibody. After washing with TBST+BSA, the sections were incubated for 1 h with protein A–gold (15 nm) diluted 1:100 with TBST+BSA. The sections were washed sequentially with TBST+BSA, TBST, and distilled water, and then post-stained with a 1:4 dilution of 1% (w/v) potassium permanganate and 2% (w/v) uranyl acetate. Images were collected using JEOL JEM-1200 EX and FEI Tecnai G2 transmission electron microscopes. The density of labelling was determined by counting the gold particles on electron micrographs and calculating the number per unit area (μm^2) with an image analysis program (ImageJ 1.37v). For each cell type, replicate measurements were made on parts of cell sections (n=10–15). Immunolabelling procedures were performed separately for different species; the difference in the labelling intensity reflects the difference between cell types but not between species. The level of background labelling was low in all cases.

Staining for polysaccharides

To reveal the localization of starch, the leaf samples were fixed in the same way as for immunolocalization, but after 15:00 h. The periodic acid–Schiff's procedure was used for staining starch in sectioned materials. Sections, 0.8–1 μm thick, were dried onto gelatin-coated slides, incubated in 1% (w/v) periodic acid for 30 min, washed, dried, and then incubated with Schiff's reagent (Sigma, St Louis, MO,

USA) for 1 h. After rinsing, the sections were ready for analysis by light microscopy. Cell walls and starch stained bright reddish pink, while other elements of the cells (cytoplasm) remained unstained. Controls lacking the periodic acid treatment (required for oxidation of the polysaccharides giving rise to Schiff's-reactive groups) showed little or no background staining (not shown).

Western blot analysis

Total soluble proteins were extracted from leaves by homogenizing 0.2 g of tissue in 0.2 ml of extraction buffer [100 mM TRIS-HCl, pH 7.5, 10 mM (w/v) $MgCl_2$, 1 mM (w/v) EDTA, 15 mM (v/v) β-mercaptoethanol, 20% (v/v) glycerol, and 1 mM phenylmethylsulphonyl fluoride]. Insoluble material was removed by centrifugation (5 min, 14 000 *g*). The supernatant fraction was diluted 1:1 in 60 mM TRIS-HCl, pH 7.5, 4% (w/v) SDS, 20% (v/v) glycerol, 1% (v/v) β-mercaptoethanol, and 0.1% (w/v) bromphenol blue, and boiled for 5 min for SDS–PAGE. Protein concentration was determined with an RCDC protein quantification kit (Bio-Rad), which tolerates detergents and reducing agents. Protein samples (20 µg) were separated by 12% SDS–PAGE, blotted onto nitrocellulose, and probed overnight at 4 °C with anti-*Amaranthus hypochondriacus* NAD-ME IgG which was prepared against the 65 kDa α-subunit, courtesy of J. Berry (Long and Berry, 1996) (1:5000), anti-*Zea mays* 62 kDa NADP-ME IgG, courtesy of C. Andreo (Maurino et al., 1996) (1:5000), anti-*Z. mays* phosphoenolpyruvate carboxylase (PEPC) IgG (1:100 000), anti-*Z. mays* pyruvate,Pi dikinase (PPDK) IgG, courtesy of T. Sugiyama (1:5000), and anti-*Spinacia oleracea* Rubisco LSU IgG (1:10 000). Goat anti-rabbit IgG–alkaline phosphatase conjugate antibody (Sigma Chemical Co.) was used at a dilution of 1:50 000 for detection. Bound antibodies were localized by developing the blots with 20 mM nitroblue tetrazolium and 75 mM 5-bromo-4-chloro-3-indolyl phosphate in detection buffer (100 mM TRIS-HCl, pH 9.5, 100 mM NaCl, and 5 mM $MgCl_2$).

CO_2 compensation point (Γ) and photosynthetic CO_2 response

For measurement of the response of photosynthesis to varying light and CO_2, and for determining the CO_2 compensation point (Γ), gas exchange was measured with a portable CO_2 analyser ADC LCPro+ (ADC BioScientific Ltd., Hoddesdon, UK). For each experiment, part of a branch of an intact plant was enclosed in the conifer chamber designed for terete or semi-terete leaves. The branch was illuminated with a PPFD of 920 µmol quanta m^{-2} s^{-1} under 370 µbar CO_2 until a steady-state rate of CO_2 fixation was obtained (generally 45–60 min). The air temperature was 25 ± 0.5 °C, the leaf temperature 27.2 ± 0.2 °C, the minimum percentage humidity in the chamber was 38 ± 1.5%, and the flow rate was 200 µmol s^{-1}. For varying light experiments at 370 µbar CO_2, measurements were made beginning at a PPFD of 1380, with decreasing levels at 4 min intervals. For varying CO_2 experiments at a PPFD of 920, the CO_2 level was first decreased, and then increased up to 1000 µmol mol^{-1} at 7 min intervals. Γ was determined at a PPFD of 920 and 25 °C by extrapolation of the initial slope of rates of CO_2 fixation (A) versus the intercellular CO_2 concentration in the leaf (C_i) through the x-axis where the net rate of CO_2 assimilation equals zero.

The leaf area exposed to incident light was calculated by taking a digital image of the part of the branch that was enclosed in the chamber, and then determining the exposed leaf area using an image analysis program (ImageJ 1.37v).

$\delta^{13}C$ values

Measures of the carbon isotope composition were determined at Washington State University on plant samples using a standard procedure relative to PDB (Pee Dee Belemnite) limestone as the carbon isotope standard (Bender et al., 1973). Leaf samples (from plants growing in the WSU School of Biological Sciences growth chamber) were dried at 60 °C for 24 h, milled to a fine powder, and then 1–2 mg were placed in a tin capsule and combusted in a Eurovector elemental analyser. The resulting N_2 and CO_2 gases were separated by gas chromatography and admitted into the inlet of a Micromass Isoprime isotope ratio mass spectrometer (IRMS) for determination of $^{13}C/^{12}C$ ratios (R). $\delta^{13}C$ values were determined where $\delta = 1000 \times (R_{sample}/R_{standard}) - 1$.

Phylogenetic analysis

Samples of *S. webbii* and *S. genistoides* were added to previously published data sets (Akhani et al., 2007; Wen et al., 2010) for the nuclear ribosomal DNA internal transcribed spacer region (ITS); samples utilized in the analysis are listed in Supplementary Appendix S1 at *JXB* online. The sequences were aligned using MUSCLE (Edgar, 2004). The aligned matrix of 110 samples and 724 aligned bases was analysed using RAxML (Stamatakis et al., 2008) with the GTR gamma model. Nine species of tribe Caroxyloneae were used as the outgroup based on previous studies (Akhani et al., 2007).

Results

General leaf anatomy and starch content

Leaf anatomy was studied in five *Salsola* species, formerly classified under section *Coccosalsola*, but representing different clades of Salsoleae and which were previously identified as having C_3-type carbon isotope composition: *S. divaricata*, *S. genistoides*, *S. masenderanica*, *S. montana*, and *S. webbii*. Figure 2 shows the leaf structure and the distribution of chlorenchyma in four species (*S. genistoides* not shown; its general features are very similar to those of *S. webbii*). Under the fluorescent microscope (Fig. 2A–D), there is red fluorescence from the chloroplast-containing tissues and blue fluorescence from all CWs, especially from the WS tissue (the blue fluorescence is typical of species of family Chenopodiaceae due to the presence of ferulic acid in the CWs; Voznesenskaya et al., 2008). There are usually two (or 2–3) layers of palisade-like chlorenchyma (which will subsequently be referred to as M) cells directly beneath the epidermis: the outer subepidermal layer (M1) and the inner layer (M2) (Fig. 2E–H). There is an often indistinct layer of relatively small BS cells around the peripheral vascular bundles in *S. masenderanica*, *S. montana*, *S. webbii* (Fig. 2E–G), and *S. genistoides* (not shown); however, there is a continuous layer of Kranz-like cells (KLCs), internal to the M cells around the whole leaf in *S. divaricata* (Fig. 2H). There is WS tissue in the centre of the leaves of all species which consists of 2–4 layers of cells with some differences in size and shape (Fig. 2A–G). The peripheral vascular bundles are situated under the chlorenchyma cells with their xylem side facing towards the outside of the leaf. The main vein is located more or less in the centre of the leaf and surrounded by the WS tissue.

A quantitative study of leaf chlorenchyma showed that in four of the *Salsola* species (*S. genistoides*, *S. masenderanica*, *S. montana*, and *S. webbii*) the cells of the outer (M1) and inner (M2) layers of the palisade M have nearly equal length (mean values of 104 µm for M1 and 118 µm for M2, see Supplementary Table S1 at *JXB* online). In *S. masenderanica*, sometimes there are a few extremely elongated palisade parenchyma cells extending through both layers of M cells (not shown). In contrast to the above species, in *S. divaricata*

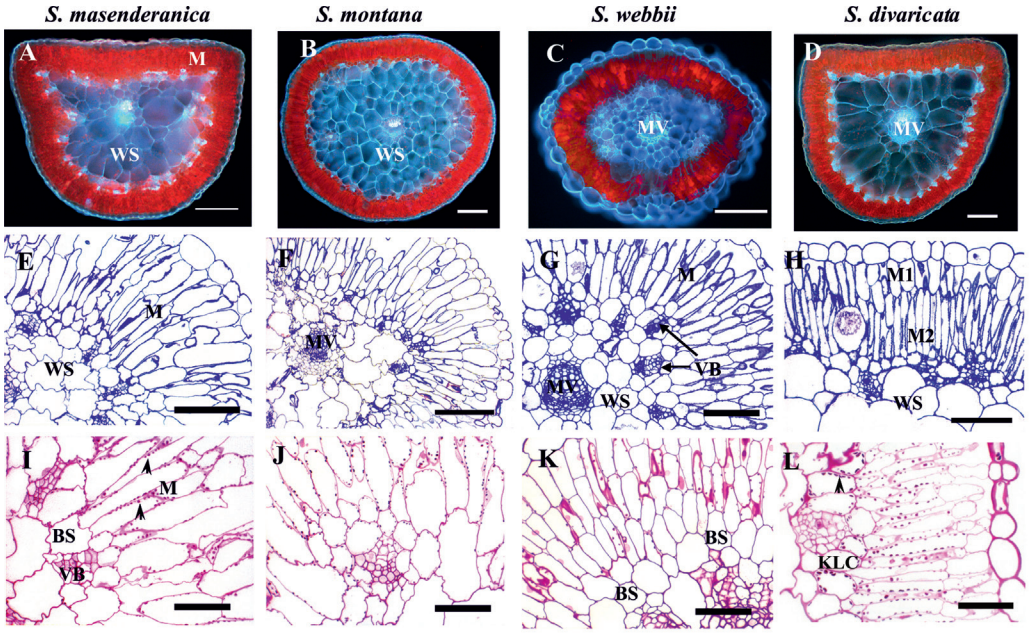

Fig. 2. Autofluorescence of leaf tissues (A–D), general anatomy (E–H), and starch localization (I–L) in leaves of four Salsoleae species of formerly *Salsola* section *Coccosalsola*. *Salsola masenderanica* (A, E, I), *S. montana* (B, F, J), *S. webbii* (C, G, K), and *S. divaricata* (D, H, L). (A–D) Autofluorescence of leaf cross-sections. (E–H) Light microscopy on leaf cross-sections showing the position of palisade mesophyll (M) and bundle sheath (BS) or Kranz-like cells (KLC). Note the continuous inner layer of KLCs in *S. divaricata* and the difference between outer (M1) and inner (M2) layers of mesophyll. (I–L) PAS (periodic acid–Schiff's) staining for carbohydrates; arrowheads point to starch grains. MV, main vein; VB, vascular bundles; WS, water storage tissue. Scale bars=200 μm for A–D, G; 100 μm for E, F, H; 50 μm for I–L.

the layer of M1 cells is much thinner than the layer of M2 cells, with a ratio of M1/M2 cell length of 0.5 similar to the hypoderm/M ratio of the two C_4 species (Supplementary Table S1). Compared with the M2 layer, the cells of the outer M1 layer of *S. divaricata* have few chloroplasts and appear more like hypodermal cells (Fig. 2H, L) which occur in some C_4 *Salsola* species. The arrangement of chlorenchyma cells in the leaf also differs between the species studied. The BS cells surrounding the peripheral vascular bundles in *S. genistoides* and *S. webbii* are not specialized and sometimes they resemble the cells of the inner layer of M or the outer layer of WS tissue, which explains why there is high variability in the size of the BS cells. In *S. masenderanica* and *S. montana*, BS cells around the peripheral vascular bundles are more diverse and, in this case, the BS cells facing outwards are more specialized. They are smaller (area between 300 μm^2 and 400 μm^2) and contain more organelles compared with the laterally arranged BS cells, which are elongated along the vein towards the phloem part (on transverse section) and thus have a larger area. This difference accounts for the high values for BS cell area in these two species (Supplementary Table S1). In *S. divaricata*, parenchyma BS cells adjacent to peripheral veins have even more advanced diversification, with the outermost cells becoming Kranz-like; and the KLCs which form a contiguous inner chlorenchyma layer on the leaf periphery are more or less similar in shape and appearance. They form clear arcs above the veins (next to the xylem) consisting of square specialized cells of nearly similar size, while between veins these KLCs are obviously larger. In the two C_4 species, *C. orientale* and *X. richteri*, the size of KCs is less variable, and they have a uniform curvilinear pattern (nevertheless, there is an ~2-fold difference in the size of the KCs between the two C_4 species studied; Supplementary Table S1).

Among the five *Salsola* species, the percentage volume densities of chlorenchyma (M and BS cells, or KLCs) and WS tissue and the portion of M versus BS or KLC tissue in the leaf were compared with the two C_4 species (from analysis of leaf cross-sections in mature leaves). In four species, *S. genistoides*, *S. masenderanica*, *S. montana*, and *S. webbii*, the chlorenchyma occupies ~60–70% (mean 64%) of leaf volume, with the main contribution from M cells, while the BS generally comprises only 4.5–6.8% of leaf volume (mean 5.5%). However, in *S. divaricata*, the chlorenchyma occupies only ~37% of leaf volume and, in comparison with the above species, invests only about half as much in the M cells, with a similar volume density of the layer of KLCs (6%). In the C_4 species studied, the chlorenchyma occupies ~30–35% of leaf volume. The ratios of volume densities of M/BS cells was high in four *Salsola* species (from 9 to 15, mean=12), compared with 5.2 for the M/KLCs in *S. divaricata*, with the lowest ratios of M/KCs in the C_4 species (2.1–4.5) (Supplementary Table S2 at *JXB* online).

The leaf volume invested in WS tissue in the four species *S. genistoides*, *S. masenderanica*, *S. montana*, and *S. webbii* is low (mean 23%, lowest in *S. webbii* and *S. genistoides*), versus 55% in *S. divaricata* versus a mean of 38% for the C_4 species (Supplementary Table S2).

The specific periodic acid–Schiff's staining for polysaccharides shows a similar density of starch staining in chloroplasts

of M and BS cells of *S. masenderanica* and *S. montana*, indicating equivalent starch storage in all chloroplasts (Fig. 2I, J). In *S. webbii* (Fig. 2K) and *S. genistoides* (not shown), there is little labelling for starch in BS cells (which is due to few chloroplasts in BS cells as shown subsequently by electron microscopy). In contrast, in *S. divaricata*, there is a gradient in starch distribution from little to no starch in the hypodermal layer (M1), with substantial starch in the inner palisade layer (M2), and with the largest starch grains in KLCs (Fig. 2L).

Results on the pattern and density of peripheral veins in the five *Salsola* species compared with the two C_4 representatives are shown in Fig. 3 and Table 1. All studied species, except for *S. genistoides*, have small peripheral veins distributed more or less evenly around the leaf under the chlorenchyma, especially in the middle part of the leaf, often with gaps on the adaxial and/or abaxial side below or above the main vein in cross-sections (Fig. 2A–D). In *S. genistoides*, peripheral veins occur in the lateral plane of the leaf and are represented by closely arranged thicker vascular bundles (not shown). Except for *S. montana*, all species have a similar pattern with a vein network consisting of a reticulate venation with rare terminal ends in minor veins; the network is elongated along the axis of the leaf. In *S. montana*, the venation consists of an elaborated reticulate network with rather numerous terminal ends (Fig. 3). The vein densities in the *Salsola* species range from ~10 mm/mm^2 to 15 mm/mm^2 while the C_4 species *C. orientale* and *X. richteri* have vein densities of 9.2 mm/mm^2 and 15 mm/mm^2, respectively. The lower densities of peripheral veins in *S. masenderanica* and *S. divaricata* are similar to that of the C_4 *C. orientale*, while the high vein density in *S. genistoides*, *S. montana* and *S. webbii* is close to that in C_4 *X. richteri* (Table 1).

Transmission electron microscopy

Figure 4 shows electron microscopy of leaf chlorenchyma for four of the '*Coccosalsola*' *Salsola* species (*S. masenderanica*, *S. montana*, *S. webbii*, and *S. divaricata*). There are differences between these in the quantity and level of development of organelles in BS cells; *S. genistoides* (not shown) has features which are very close to those of *S. webbii*. *Salsola masenderanica* (Fig. 4A, B) and *S. webbii* (Fig. 4I, J) have the lowest occurrence of chloroplasts and mitochondria in BS cells; *S. montana* have a thicker cytoplasmic layer with more organelles in BS cells (Fig. 4E, F), while the KLCs in *S. divaricata* contain numerous chloroplasts and mitochondria (Fig. 4M, N).

In *S. masenderanica* (Fig. 4A), *S. webbii* (Fig. 4I), and *S. genistoides* (not shown) chloroplasts and mitochondria are distributed more or less evenly around the CWs, with some mitochondria also located in a centrifugal position. However, in the BS cells of *S. montana* and KLCs of *S. divaricata*, while the chloroplasts are distributed around the CWs, most of the mitochondria are located close to the inner periclinal or radial CWs (Fig. 4E, F, M–O).

Bundle sheath (Fig. 4C, G, K, O) and M (Fig. 4D, H, L, P) chloroplasts in all five species have a similar structure with a well-developed system of medium sized grana. The mitochondria in BS and M cells in *S. genistoides*, *S. masenderanica*, *S. montana*, and *S. webbii* have a similar size and structure (0.3–0.5 µm; Table 2, Fig. 4B, F, J for BS mitochondria); but, in *S. divaricata* the KLC mitochondria are larger (average 0.6 µm; Table 2) and they have a more elaborated system of cristae (Fig. 4N, O). The KC mitochondria of *C. orientale* (an NAD-ME-type C_4 species), which are 2.3 times larger than in M cells, are about the same size as the KLC mitochondria in *S. divaricata* (Table 2), and they are distributed

Table 1. *Vein density in representative* Salsola *s.l. species*

Species	Vein density (mm/mm^2)
S. masenderanica	10.0±0.5
S. montana	15.0±0.5
S. webbii	12.5±0.6
S. divaricata	10.3±0.4
C. orientale	9.2±0.8
X. richteri	15.0±0.5

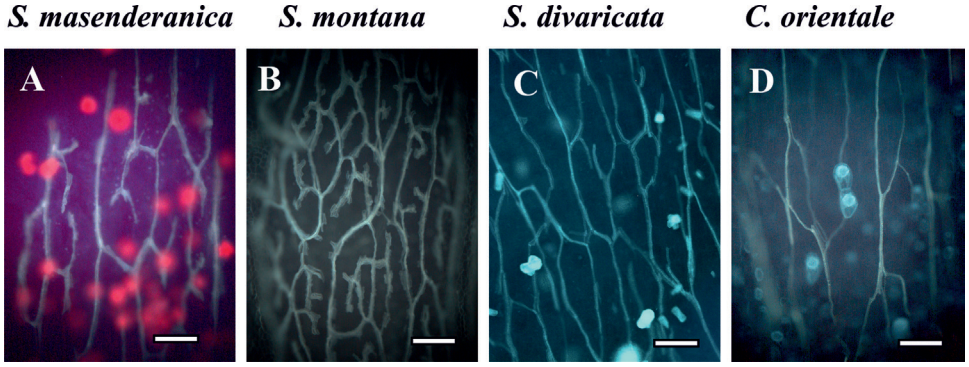

Fig. 3. Illustration of the venation pattern and leaf vein density on cleared leaves of three Salsoleae species of formerly *Salsola* section *Coccosalsola*, *Salsola masenderanica* (A), *S. montana* (B), *S. divaricata* (C), and the C_4 Salsoloid-type species *Caroxylon orientale* (D). Observation of cleared leaves under UV light shows a low branching pattern with few terminal ends and low density of the veins in three species, *S. masenderanica* (A), *S. divaricata* (C), and *C. orientale* (D), and a higher density of branched veins in *S. montana* (B). Scale bars=200 µm.

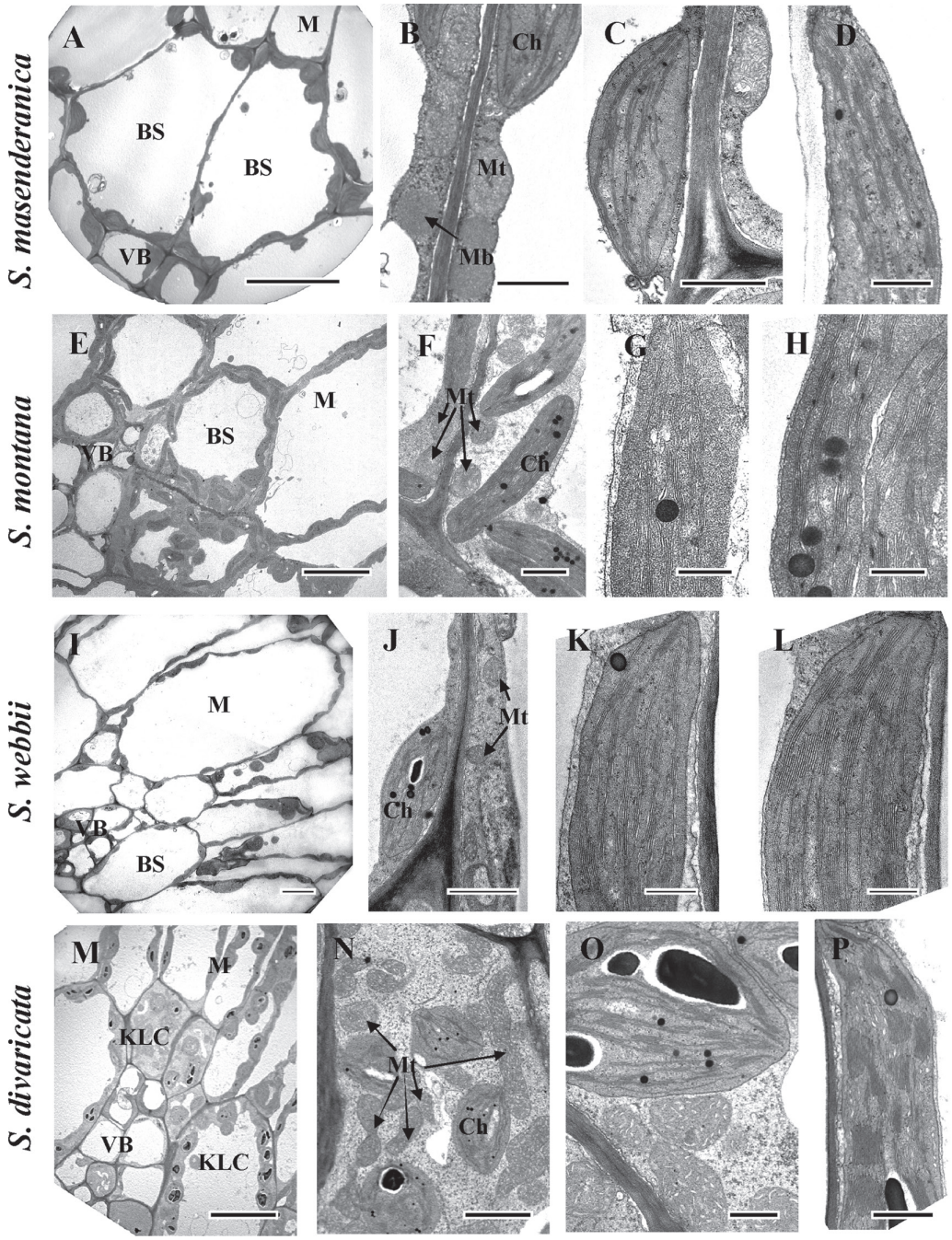

Fig. 4. Electron microscopy of mesophyll (M) versus bundle sheath (BS) and Kranz-like cells (KLCs) in leaves of four Salsoleae species of formerly *Salsola* section *Coccosalsola*: *S. masenderanica* (A–D), *S. montana* (E–H), *S. webbii* (I–L), and *S. divaricata* (M–P). (A, E, I, M) Micrographs show M and BS/KLCs around vascular bundles. (B, F, J, N, O) Organelles in BS and KLCs at a higher magnification. Note the difference in abundance of organelles in BS and KLCs between species, and the numerous mitochondria in KLCs of *S. divaricata* (N, O). (C, G, K, O) Chloroplast structure in BS and KCLs of the four species. (D, H, L, P) Structure of M chloroplasts in the four species. Ch, chloroplast; Mb, microbody; Mt, mitochondria; VB, vascular bundle. Scale bars=10 μm for A, E, I, M; 1 μm for B, C, F, J; 0.5 μm for D, G, H, K, L, O, P; and 2 μm for N.

in a centripetal position, close to the vascular bundles (not shown). The KC mitochondria of *X. richteri*, an NADP-ME-type C_4 species, which are also distributed in a centripetal position, are small (not shown) and similar in size to BS mitochondria of *S. genistoides*, *S. masenderanica*, *S. montana*, and *S. webbii* (Table 2).

Table 3 shows results on the thickness of CWs of chlorenchyma cells where they are exposed to the intercellular air space (IS), the M and BS cells of *S. genistoides*, *S. masenderanica*, *S. montana*, and *S. webbii*, the M cells and KLCs of *S. divaricata*, and the M cells versus KCs of the C_4 species *X. richteri.* Among the *Salsola* species, for thickness of BS

Table 2. *Mitochondrial size (small diameter) in representative* Salsola *s.l. species*

Species	Mitochondrial size (µm)	
	BS, KLC, or KC	M
S. genistoides	0.45 ± 0.02	0.40 ± 0.02
S. masenderanica	0.32 ± 0.03	0.36 ± 0.02
S. montana	0.44 ± 0.01	0.43 ± 0.03
S. webbii	0.38 ± 0.02	0.51 ± 0.02
S. divaricata	0.62 ± 0.02	0.38 ± 0.03
C. orientale, C_4	0.65 ± 0.04	0.32 ± 0.02
X. richteri, C_4	0.39 ± 0.04	0.47 ± 0.01

BS, bundle sheath cells around veins; KCL/KC, inner layer of Kranz-like or Kranz cells, M, mesophyll cells.

cell/KLC/KC CWs exposed to the IS, *S. divaricata* had the highest value (0.31 µm), which was 1.5- to 3-fold higher than that of the other species; while this value for the C_4 *X. richteri* was much higher (2.9 µm).

The thickness of CWs exposed to the IS is shown for the subepidermal M1 versus the inner M2 cells. In the M1 cells (which are specialized hypodermal cells in *X. richteri*), the thickness of the CWs exposed to the IS ranged between 0.11 µm and 0.20 µm, with the highest values in *S. divaricata* and the C_4 *X. richteri.* In three species, *S. genistoides*, *S. divaricata*, and C_4 *X. richteri*, the subepidermal M1 cells have thicker CWs than the M2 cells, being slightly thicker in *S. genistoides*, ~1.5 times thicker in *X. richteri*, and up to ~3 times thicker in *S. divaricata*. The thickness of M2 CWs exposed to the IS was similar and low among the species, ranging from 0.07 µm to 0.12 µm.

Among the five *Salsola* species, the combined thickness of the BS or KLC CWs in contact with other cells (M or BS/KLCs) ranged from 0.20 to 0.29, while in C_4 *X. richteri* these values for KCs in contact with M cells or other KCs were much higher (2.42 in contact with M cells and 0.97 µm in contact with other KCs). Among the *Salsola* species, the combined thickness of the KLCs in contact with WS cells in *S. divaricata* (0.73 µm) was 2- to 6-fold higher than in other *Salsola* species; while the C_4 *X. richteri* had the highest value (1.52 µm).

Western blot analysis

Immunoblots for Rubisco, and for key C_4 cycle enzymes PEPC, PPDK, NAD-ME, and NADP-ME from total soluble proteins extracted from leaves of the studied species are presented in Fig. 5. The carboxylase of the C_3 pathway, Rubisco, analysed by western blots with the large subunit antibody, is abundant in all species. The C_4 species *X. richteri* and *C. orientale* have very high labelling of the C_4 pathway enzymes, PEPC and PPDK, with difference in abundance of the two malic enzymes. *Xylosalsola richteri* has clear labelling for NADP-ME and lower labelling for NAD-ME, while *C. orientale* has strong labelling for NAD-ME, and no detectable labelling for NADP-ME. Compared with the two C_4 species, the five *Salsola* species, *S. genistoides*, *S. masenderanica*, *S. montana*, *S. webbii*, and *S. divaricata*, have no labelling for the C_4 cycle enzymes PPDK and NADP-ME, very low labelling for PEPC, and to varying degrees less labelling for NAD-ME (lowest in *S. webbii*, highest in *S. divaricata*).

Carbon isotope composition

The focus of this study is on five species of the tribe Salsoleae (formerly classified under section *Coccosalsola*) where C_3-type carbon isotope composition, and/or lack of Kranz-type anatomy has been recognized (see the Introduction). Leaves of plants of *S. genistoides*, *S. masenderanica*, *S. montana*, *S. webbii*, and *S. divaricata* grown in the current study have C_3-type isotope composition with mean $\delta^{13}C$ values between –22.6‰ and –29.7‰ (Table 4; see also Table 5 for values for these species from previous reports). Comparative values for the C_4 species *C. orientale* and *X. richteri* were –13.5‰

Table 3. *Thickness of cell walls in leaf cross-sections of representative* Salsola *s.l. species*

Species	A. Thickness of individual cell walls towards the IS (µm)			B. Combined thickness of adjacent cell walls (µm)		
	BS, KLC, KC	M1	M2	BS, KLC or KC in contact with other cells		
	Towards M IS	Towards IS	Towards IS	M	BS, KLC, KC	WS
S. genistoides	0.20 ± 0.005	0.16 ± 0.003	0.12 ± 0.004	0.21 ± 0.011	0.26 ± 0.008	0.36 ± 0.017
S. masenderanica	0.19 ± 0.007	0.13 ± 0.003	0.11 ± 0.003	0.22 ± 0.002	0.20 ± 0.02	0.13 ± 0.03
S. montana	0.11 ± 0.01	0.11 ± 0.005	0.11 ± 0.003	0.24 ± 0.011	0.25 ± 0.01	0.19 ± 0.02
S. webbii	0.17 ± 0.004	0.12 ± 0.004	0.10 ± 0.002	0.29 ± 0.008	0.29 ± 0.012	0.14 ± 0.004
S. divaricata	0.31 ± 0.01	0.20 ± 0.01	0.07 ± 0.002	0.29 ± 0.013	0.24 ± 0.02	0.73 ± 0.02
X. richteri, C_4	2.9 ± 0.22	0.18 ± 0.01[a]	0.11 ± 0.004[b]	2.42 ± 0.12	0.97 ± 0.03	1.52 ± 0.12

BS, bundle sheath cells surrounding veins; KC, KLC, internal layer of Kranz or Kranz-like cells; IS, intercellular air space; M, mesophyll cell; WS, water storage cell.

In each case *n*=15–30 measurements. Values are shown with standard errors.

[a] For *X. richteri*, this layer represents specialized hypoderm.

[b] For *X. richteri*, this layer could be also referred as M.

(A) Thickness of individual cell walls of BS, KLC, or KC, M1 (or hypodermal cells in *Xylosalsola richteri* and hypodermal-like in *S. divaricata*), or M2 cells when in contact with intercellular air space. (B) Combined thickness of cell walls where BS cells, KLCs, or KCs are in contact with other cells (M, WS, or an adjacent BS, KLC or KC).

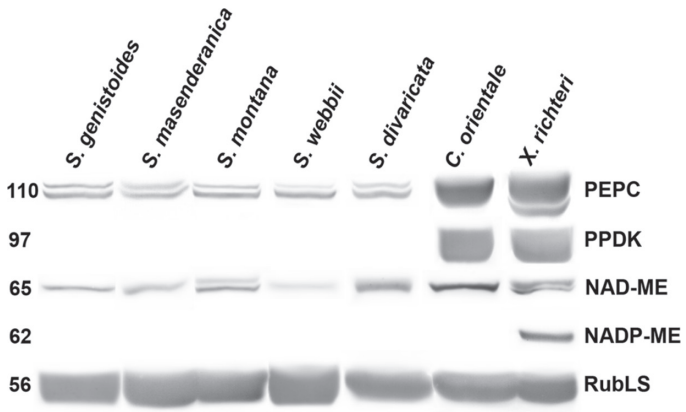

Fig. 5. Western blots for C_4 enzymes and Rubisco from soluble proteins extracted from leaves of five *Salsola* species s.l., *Salsola genistoides*, *S. masenderanica*, *S. montana*, *S. webbii*, and *S. divaricata*, and two C_4 Salsoloid-type species, *Caroxylon orientale* and *Xylosalsola richteri*. Blots were probed with antibodies raised against PEPC, PPDK, NAD-ME, NADP-ME, and Rubisco large subunit, respectively. Numbers on the left indicate the molecular mass in kiloDaltons.

Table 4. *Carbon isotope composition of leaf biomass ($\delta^{13}C$) and CO_2 compensation point (Γ) at 25 °C and 920 PPFD in representative* Salsola *s.l. species*

Average numbers of several measurements are presented; for $\delta^{13}C$ individual numbers and sources, see Table 5.

Species	Carbon isotope composition ($\delta^{13}C$)	CO_2 compensation point (Γ, ppm)
S. genistoides	–29.7 ± 1.00	46.3 ± 0.2 (*n*=2)
S. mazenderanica	–23.6 ± 0.06	74.9 ± 1.8 (*n*=6)
S. montana	–22.6 ± 0.03	52.8 ± 6.1 (*n*=4)
S. webbii	–24.5 ± 0.10	49.7 ± 0.1 (*n*=4)
S. divaricata	–29.2 ± 0.17	32.3 ± 2.9 (*n*=6)
C. orientale	–13.5 ± 0.46	5.5 ± 1.5 (*n*=5)
X. richteri	–12.1 ± 0.04	5.8 ± 0.9 (*n*=4)

to –12.1‰, respectively. Table 5 is a summary of the carbon isotope composition of plant samples, and type of anatomy where known, of species in this group (combining the present analysis with some previous data). The results show that 18 species have C_3-type isotope values (*S. abrotanoides*, *S. arbusculiformis*, *S. botschantzevii*, *S. deschaseauxiana*, *S. divaricata*, *S. drobovii*, *S. genistoides*, *S. flexuosa*, *S. gymnomaschala*, *S. junatovii*, *S. laricifolia*, *S. lipschitzii*, *S. masenderanica*, *S. montana*, *S. oreophila*, *S. pachyphylla*, *S. tianshanica*, and *S. webbii*) and 18 species have C_4 isotope values.

Gas exchange measurements

Light and CO_2 response curves of photosynthesis were measured for comparison of the *Salsola* species with the C_4 plants *C. orientale* and *X. richteri.* The light response curves measured under atmospheric levels of CO_2 (370 µmol mol^{-1}) at 25 °C show that the C_4 species *X. richteri* and *C. orientale* have increasing rates of CO_2 fixation up to 1400 PPFD, whereas the three *Salsola* species become light saturated at lower PPFD. The maximum rates of photosynthesis in the two C_4 species were higher than in the *Salsola* species *S. masenderanica*, *S. montana* (Fig. 6A), *S. genistoides*, and *S. webbii* (not shown). Maximum rates in *S. divaricata* were closer to that of the C_4 species (Fig. 6A).

The Γ values determined from CO_2 response curves at 25 °C, 920 PPFD, and atmospheric O_2 (21%) were 5.5 µbar and 5.8 µbar for the C_4 species *C. orientale* and *X. richteri.* Among the *Salsola* species, *S. divaricata* had a low Γ value (32.3 µbar), compared with an average value of ~50 µbar for three species (*S. genistoides*, *S. webbii*, and *S. montana*), while *S. mazenderancia* had a higher value (Table 4). Plots of CO_2 assimilation rates versus increasing intercellular levels of CO_2 show that the C_4 species *X. richteri* and *C. orientale* have a rapid increase in rate approaching saturation at a C_i of ~300 µbar CO_2, whereas *S. masenderanica*, *S. montana*, *S. divaricata* (also *S. genistoides* and *S. webbii*, not shown) had a C_3-like response, with photosynthesis continuing to increase up to ~600 µbar CO_2 (Fig. 6B).

Immunolabelling for GDC

In situ immunolabelling for GDC using the antibody to the P protein was examined by electron microscopy, and quantitative analysis made based on the density of gold particles, in four of the *Salsola* species *S. masenderanica*, *S. montana*, *S. webbii*, and *S. divaricata*, and compared with that in the C_4 species *C. orientale.* Analysis of the immunolabelling distribution shows that there is no significant difference in density of the gold particles between the mitochondria of M and BS cells in *S. masenderanica*, *S. montana*, and *S. webbii* (Fig. 7). In contrast, in *S. divaricata*, the number of gold particles is 7.5 times higher in the KLC compared with M mitochondria. In the C_4 species *C. orientale*, gold particles are also selectively localized in the KC mitochondria, with low labelling in M mitochondria (Fig. 7).

Phylogenetic analysis

The tree depicted in Fig. 8 shows the maximum likelihood phylogenetic analysis of tribe Salsoleae based on ITS sequence data. The colour coding shows species studied herein, belonging formerly to section '*Coccosalsola*', including the five *Salsola* species of interest (*S. genistoides*, *S. masenderanica*, *S. montana*, *S. webbii*, and *S. divaricata*), *S. arbusculiformis*, *S. laricifolia*, and the C_4 species *X. richteri*, *X. arbuscula*, and *X. chivensis*, *S. foliosa* and *S. zygophylla*; and, in addition, three other species (*Salsola* '*touranica*', *Sympegma regelii*, and *Raphidophyton regelii*). All of these, other than the C_4 species, are known to be species with C_3-type isotope composition and/or non-Kranz anatomy. The positions of the two known C_3–C_4 intermediates are highlighted (blue). The results found here closely reflect the results of previous studies (Akhani et al., 2007; Wen et al., 2010). This is the first study to find strong support for *S. webbii* and *S. genistoides* forming a grade with *Sympegma* leading to the rest of the tribe.

Table 5. *Data on carbon isotope composition and leaf anatomy of species formerly classified under* Salsola *section* Coccosalsola

Some species are placed in the informal clade '*Oreosalsola*' based on morphological features (HA, unpublished); additional analysis by molecular phylogeny is needed.

Species	Source[a]	$\delta^{13}C$ leaf	Reference	Leaf structure	Reference
'Canarosalsola'					
S. divaricata Masson ex Link	LE	–24.5	Pyankov et al. (2001*b*)	Kranz-like Sals	This study
	WSU	–28.9, –29.7	This study		
	Canary Islands, Tenerife, H. Freitag 10.319 (KAS)	–25.7, –25.5	This study		
'Collinosalsola'					
S. arbusculiformis Drobow	Iran	–24.0	Akhani et al. (1997)	Symp	Butnik *et al.* (1991)
	Uzbekistan	–21.2, 26.8	Pyankov et al. (1997)	Symp	Pyankov et al., (1997)
	LE	–23.9	Pyankov et al. (2001*b*)	Symp	Pyankov et al. (2001*b*)
	Iran	–24.0, –28.9	Akhani and Ghasemkhani (2007)	C_3–C_4 Kranz-like Symp	Voznesenskaya et al. (2001) This study
S. laricifolia Turcz. & Litv.	LE	–23.1	Pyankov et al. (2001*b*)	C_3–C_4 Symp	Wen and Zhang (2011)
	China	–22.1	Wen and Zhang (2011)	Kranz-like Sals	This study
	Kazakstan, S. Lipschitz, 7.09.1928 (MW)	–20.6	This study		
	Kazakstan, I.A. Gubanov, 30.07.1959 (MW)	–25.3	This study		
'Oreosalsola'					
S. abrotanoides Bunge	LE	–24.9	Pyankov et al. (2001*b*)	Symp	Pyankov et al. (2001*b*)
	China, T.N. Ho *et al*., 3129, 18.09.96, (MO)	–24.7, –24.5	This study		
	Mongolia, V.I. Grubov *et al*., 1182, 25.08.1972, (LE)	–24.0, –23.6	This study		
S. botschantzevii Kurbanov	LE	–22.7	C.C. Black, personal communication		
S. drobovii Botsch.	LE	–24.4	Pyankov et al. (2001*b*)	Kranz-like Sals	This study
	Kirgizia, V.B. Kuvaev,#153, 4.09.1960. Det. A. Elenevskii (MW)	–26.1	This study		
S. flexuosa Botsch.	Kirgizia, V. Botschantzev, #335, 26.07.1974 (LE)	–23.3, –23.5	This study		
S. gymnomaschala Maire	SW Morocco, H. Freitag, 35.019 (KAS)	–27.8, –27.8	This study		
	Marocco, R. Maire, 31.03.1937 (LE)	–25.3, –25.1	This study		
S. junatovii Botsch.	China, A.A. Junatov, J.Ifen, 143.7 Ju, 31.07.1968 (LE)	–21.1, –21.9	This study		
S. lipschitzii Botsch.	S. Uzbekistan, V. Botschanzev, 26, 9.06.1971 (LE)	–24.0	This study		
S. masenderanica Botsch.	LE	–22.2	Pyankov et al. (2001*b*)	Symp	This study
	WSU	–23.5, –23.6	This study		
S. montana Litv.	Iran	–25.74	Akhani et al., (1997)	Symp	Butnik, (1984)
	Uzbekistan	–27.2, –26.8, –28.4	Pyankov et al. (1997)	Symp	Pyankov et al. (2001*b*); Akhani and Ghasemkhani, (2007)
	LE	–22.8	Pyankov et al. (2001*b*)	Proto-Kranz	This study
	Iran	–26.3	Akhani and Ghasemkhani (2007)		
	WSU	-22.5, 22.6	This study		
S. oreophila Botsch.	West Pamirs, Vanch River	–27.2	Pyankov et al. (1997)	Symp	Pyankov et al. (1997)
	Pamirs Moutain, Badachshan region, K. Stanyukovitsch *et al*., 8008, 5.07.1958 (LE)	–21.5, –21.9	This study		
S. pachyphylla Botsch.	Uzbekistan	–24.6	Pyankov et al. (1997, 2001*b*)	Symp	(Butnik (1984)
S. tianschanica Botsch.	LE	–20.4	Pyankov et al. (2001*b*)		
Salsola s.s.					
S. cruciata Chevall.	Libya, Agedabia, U. Pratov, 10 October 1978 (LE)	–10.5, –10.3	This study		
S. cyrenaica (Maire et Weiller) Brullo	Libya, Cirenaica, Wadi Derna S. Brullo & Furnari 16.09.1974 (KAS)	–14.4, –13.8	This study		

Table 5. Continued

Species	Source[a]	$\delta^{13}C$ leaf	Reference	Leaf structure	Reference
S. cyrenaica (Maire et Weiller) Brullo subsp. *antalyensis*	S Turkey, Antalya Prov., H. Duman, no. 6838, 08.08.1998 (KAS)	–15.9, –15.6	This study		
S. drummondii Ulbr	Iran, H. Akhani 6727	–12.14	Akhani et al. (1997)	Sals (+H)	This study
	Pakistan, Baluchistan, H. Freitag, no. 18535, 01.10.1986 (KAS)	–13.2, –14.0	This study	Sals (–H)	Butnik (1976)
S. foliosa (L.) Schrad. ex Schult.	Turkmenistan	–12.0	Akhani et al. (1997)		
S. kerneri (Wol.) Botsch.	LE	–11.4	Pyankov et al. (2001*b*)		
	Iran	–12.9	Akhani et al. (1997)		
	LE	–11.1	Pyankov et al. (2001*b*)		
S. longifolia Forssk.	–	–14.7	Winter (1981)	Sals (+H)	Carolin et al. (1975)
	LE	–12.4	Pyankov et al. (2001*b*)		
S makranica Freitag	Pakistan, Baluchistan, H. Freitag, no.18.587, 05.10.1986 (KAS)	–11.1, –11.3	This study		
S. melitensis Botsch.	Malta, Gozo, M. Appelhans 02.08.2007 (KAS)	–6.9, –7.1	This study		
S. oppositifolia Desf.	–	–13.2	Winter (1981)		
	Spain	–11.14	Akhani et al. (1997)		
	LE	–12.5	Pyankov et al. (2001*b*)		
	Espagne, E. Evrard, 11.57, 25.05.1991 (MO)	–13.0, –12.6	This study		
	Algeria, A. Dubuis, 12079, 27.07.1985 (MO)	–14.6	This study		
	Morocco, S. Castroviejo, J. Fdez. Casas, F. Munoz Garmendia, A. Susanna, FC5174, 27.05.1981 (under the name *S. verticillata*) (MO)	–11.3, –12.4	This study	Sals	This study
	Spain, Mallorca, 4.6.1987 (under the name *S. verticillata*), (# PO5072854, P)	–11.7, –12.1	This study		
	S. Spain, Almeria, M. Costa, No. 12973, 4.11.1984 (#P05344398, P)	–11.4, –11.1	This study		
S. schweinfurthii Solms	–	–12.9	Winter (1981)		
	Palestine	–14.1	Akhani et al. (1997)		
	LE	–12.0	Pyankov et al. (2001*b*)		
S. verticillata Schousb.	Morocco, Prov. de Safi, D. Podlech, 44954, 23.4.1989 (#P05267738, P)	–11.2, –11.2	This study		
S. zygophylla Batt. & Trab.	–	–13.0	Winter (1981)		
	Algeria	–10.2	Akhani et al. (1997)		
	LE	–11.7	Pyankov et al. (2001*b*)		
Xylosalsola					
X. arbuscula (Pall.) Tzvelev (=*S. arbuscula* Pall)	Uzbekistan, Mongolia	–13.0, –12.9	Pyankov et al. (1997)	Sals (+H)	Rojanovskii (1970)
	Iran	–12.4	Akhani et al. (1997	Sals (+H)	Voznesenskaya et al., (2001)
				Sals (+H)	Butnik *et al.* (1991)
X. chiwensis (Popov) Akhani & Roalson (*S. chiwensis* Popov)	LE	–12.4	Pyankov et al. (2001*b*)		
S. euryphylla Botsch.[b]	Kazakstan, A. Yunatov, L. Kuznezov, 24.07.1956 (LE)	–11.4, –11.6	This study	Sals	Butnik (1984)
X. paletzkiana (Litv.) Akhani & Roalson (*S. paletzkiana* Litv.)	–	–12.9	Winter (1981)	Sals (+H)	Carolin et al. (1975)
	WSU	–13.3, –13.2	This study	Sals (+H)	Butnik (1984)
				Sals (+H)	Butnik *et al.* (1991)

Table 5. Continued

Species	Source[a]	$\delta^{13}C$ leaf	Reference	Leaf structure	Reference
X. richteri (Moq.) Akhani & Roalson	–	–11.9	Winter (1981)	Sals (+H)	Carolin et al. (1975)
(=*S. richteri* (Moq.) Kar. ex Litv.)	Iran	–12.9	Akhani et al. (1997)	Sals (+H)	Voznesenskaya (1976)
	Uzbekistan	–12.9, –12.0	Pyankov et al. (1997)	Sals (+H)	Pyankov et al. (2001*b*)
	Uzbekistan	–13.6	This study	Sals (+H)	Pyankov et al. (2000)
	Uzbekistan	–12.9, –13.0	Pyankov et al. (2000)	Sals (+H)	Butnik *et al.* (1991)
		–12.9	Pyankov et al. (2001*b*)		
S. transhyrcanica Iljin[b]	LE	–11.2	Pyankov et al. (2001*b*)		
Not assigned					
S. deschaseauxiana Litard et Maire)	W Morocco, H. Freitag, 35.002 (KAS)	–26.2, –27.0	This study		
	Morocco, Agadir, H. Humbert, July 1925 (LE)	–24.6, –23.7	This study		
S. genistoides Juss. ex Poir.	Spain	–26.9	Akhani et al. (1997)	Sals	Carolin et al. (1975)
	LE	–25.0	Pyankov et al. (2001*b*)	Symp	Voznesenskaya (1976)
	WSU	–30.7, –28.7	This study	Symp	This study
S. webbii Moq.	Morocco	–26.9	Winter (1981)	Symp	Carolin et al. (1975)
	Iran	–26.8	Akhani et al. (1997)	Symp	Pyankov et al. (2001*b*)
	LE	–23.4	Pyankov et al. (2001*b*)	Symp	This study
	WSU	–24.6, –24.4	This study		

KAS, University of Kassel, Germany; LE, Herbarium of the Komarov Botanical Institute, Saint-Petersburg, Russia; MO, Herbarium of the Missouri Botanical Garden, St Louis, MO, USA; MW, Herbarium of the Moscow State University, Moscow, Russia; P, Herbarium of the Museum national d'Histoire naturelle, Paris, France; WSU, grown at the Washington State University, voucher specimen available at the WSU Marion Ownbey Herbarium, Pullman, WA, USA; Symp, Sympegmoid-type anatomy; Kranz-like Symp; Kranz-like Sympegmoid anatomy; Kranz-like Sals, Kranz-like Salsoloid anatomy; Sals, Salsoloid; +H, hypoderm is present; –H, hypoderm is absent.

[a] Information when available includes a listing of the herbarium, collector, specimen number, date, and country of origin.

[b] *Salsola euryphylla* Botsch. and *S. transhyrcanica* are presumed to belong to the *Xylosalsola* clade, but have not been included in any phylogenetic analyses and do not have a combination as of yet in *Xylosalsola*.

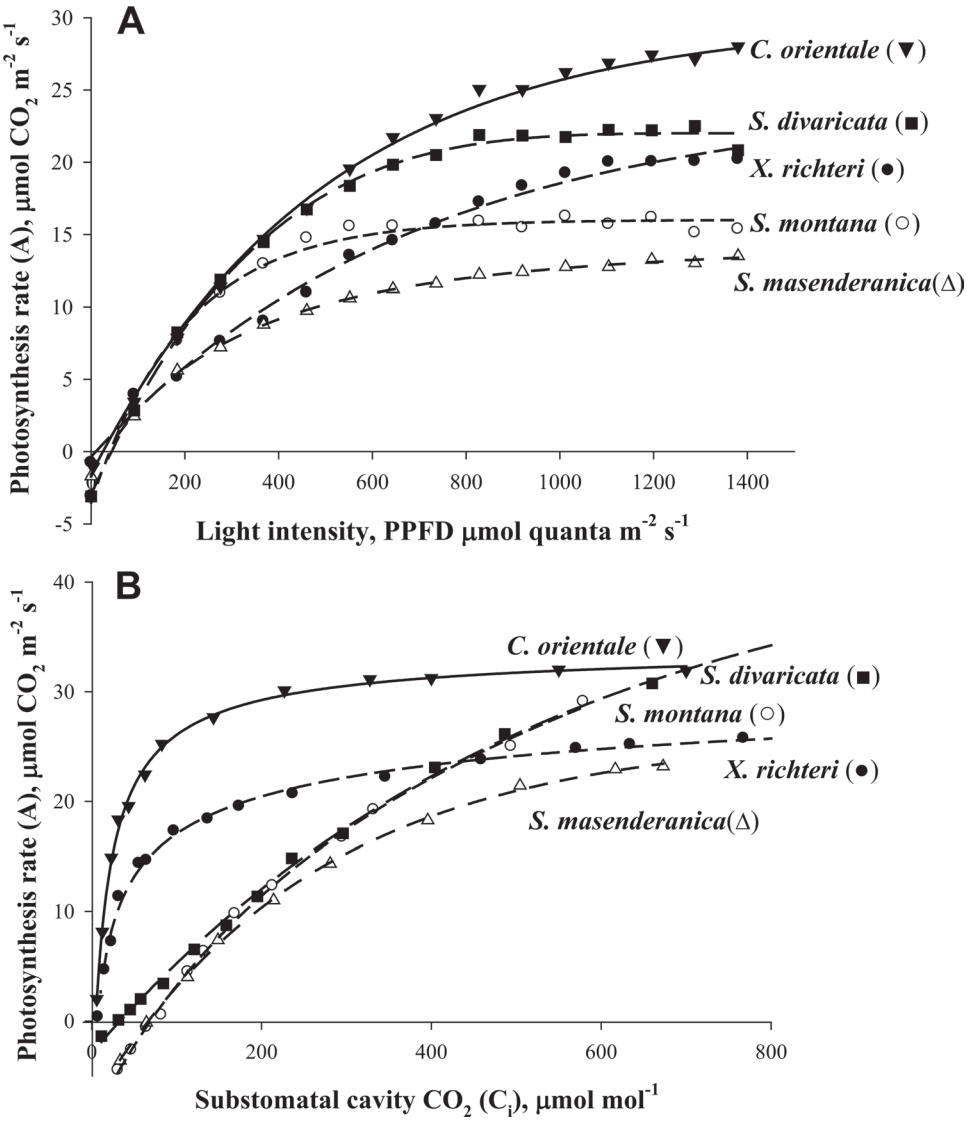

Fig. 6. Rates of CO_2 fixation in response to varying light intensity (A) and intercellular levels of CO_2 (B) in three *Salsola* species s.l., *S. masenderanica*, *S. montana*, and *S. divaricata*, and two C_4 Salsoloid-type species, *Caroxylon orientale* and *Xylosalsola richteri*. The results show the average from measurements of the response to changes in light (from high to low), and CO_2 (from ambient to low, and low to high), from 2–4 separate measurements on branches from different plants.

Discussion

Currently most known *Salsola* species having C_3-like values of carbon isotope composition occur in what was originally described as section *Coccosalsola* (Botschantzev, 1976, 1985, 1989). Among the five *Salsola* species in this study, *S. masenderanica* and *S. montana* (together with previously studied *S. arbusculiformis*) belong to subsection *Arbusculae*, *S. genistoides* and *S. webbii* belong to subsection *Genistoides*, and *S. divaricata* belongs to subsection *Coccosalsola* (Botschantzev, 1976, 1985). However, according to nuclear and chloroplast sequence data, these species do not form a monophyletic group and the following informal clade names were applied to the distinct lineages: '*Collinosalsola*' for *S. arbusculiformis*, '*Oreosalsola*' for *S. masenderanica* and *S. montana*, and '*Canarosalsola*' for *S. divaricata* (Akhani et al., 2007) (Table 6). The position of *S. genistoides* and *S. webbii* in the phylogenetic tree clearly suggests that they also do not belong to *Salsola* sensu stricto (s.s.); geographically, they are from the Mediterranean area. *Salsola genistoides* prefers arid south hill slopes; this species is an endemic of Spanish provinces Almería, Murcia, and Alicante along the Iberian Peninsula. *Salsola webbii* is distributed on the alkaline soils of sunny arid slopes of coastal mountains in Morocco and Spain (Castroviejo and Luceño, 1990). *Salsola masenderanica* and *S. montana* are distributed through the Irano-Turanian area, but *S. montana* also occurs in the lower montane zone of the Central Asian area. *Salsola montana* often grows in gypsum, marl, calcareous, and slightly salty soils (Akhani and Ghasemkhani, 2007), and *S. masenderanica* occurs in similar habitats in Alborz Mount. *Salsola divaricata* is an endemic species from the Canary Islands, which grows in semi-arid rocky zones near coastal areas (Fritzsch and Brandes, 1999; Delgado et al., 2006; and observation by

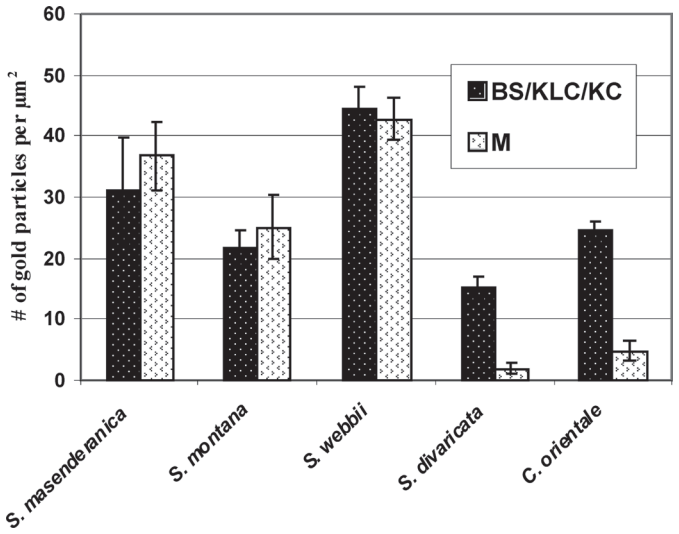

Fig. 7. Graphs showing quantitative data obtained from electron microscopy of *in situ* immunolocalization of glycine decarboxylase (GDC) in mesophyll (M) versus bundle sheath (BS) of *Salsola* species s.l., *S. masenderanica*, *S. montana*, and *S. webbii*, M versus Kranz-like cells (KLCs) of *S. divaricata* in section *Coccosalsola*, and M versus Kranz cells (KCs) in the C_4 Salsoloid-type species *Caroxylon orientale*. The density of labelling (number of gold particles per μm^2 of mitochondrial area) for GDC in mitochondria in the chlorenchyma cell types is shown. For each cell type, 10–15 cell fragments were used for counting.

HA). Most other species having C_3-type carbon isotope composition in Salsoleae, together with the previously identified C_3–C_4 intermediate species *S. arbusculiformis*, are distributed throughout the Irano-Turanian and Central Asian areas, often on slopes of hills. In formerly section *Coccosalsola*, the C_4 species which have been previously studied are NADP-ME type with Salsoloid-type Kranz anatomy (see the scheme in Pyankov et al., 1997). They occur almost continuously in arid and semi-arid zones of the Mediterranean, N African, SW and Central Asian areas.

Determination of type of photosynthesis

Gas exchange analyses of the five *Salsola* species shows that *S. genistoides*, *S. masenderanica*, *S. montana*, *S. webbii*, and *S. divaricata* are not functioning as C_4 plants since photosynthesis is saturated at lower light levels, and higher levels of CO_2 are required for saturation compared with the two representative C_4 Salsoloideae species. An important functional test for whether a species may be functioning as a C_3–C_4 intermediate is the CO_2 compensation point, since Γ values lower than that of C_3 plants are indicative of a reduction in photorespiration (Edwards and Ku, 1987). Previously, *S. arbusculiformis* was identified as the first C_3–C_4 intermediate in family Chenopodiaceae; at 25 °C it has a Γ value of 36.7 µbar compared with 5 µbar for the C_4 species *X. arbuscula* (Voznesenskaya et al., 2001). C_3 plants have minimum Γ values of ~45 ppm at 25 °C and 21% O_2, which is similar to that predicted from kinetic properties of spinach Rubisco (Woodrow and Berry, 1988). In the present study, *S. divaricata* has a lower than expected Γ value (32 µbar) suggestive of a C_3–C_4 intermediate. Values of *S. genistoides*, *S. montana*, and *S. webbii* were within the range expected of C_3 plants (46–53 µbar); while the value was higher in *S. masenderanica* (74.9 µbar). At a given temperature, higher than predicted Γ can occur depending on the rate of dark-type respiration relative to the rate of CO_2 assimilation (Furbank et al., 2009).

In C_3–C_4 intermediates, the proof of compartmentation to support refixation of photorespired CO_2, and intermediate-type Γ values comes from analysis by immunolocalization of GDC levels in BS/KLC versus M mitochondria (Rawsthorne et al., 1988; Voznesenskaya et al., 2001). *Salsola divaricata*, like the C_4 species *C. orientale*, has selective compartmentation of GDC in KLC mitochondria, as shown by quantifying the number of gold particles from immunolocalization, while in *S. masenderanica*, *S. montana*, and *S. webbii* the labelling is nearly equal in both BS and M mitochondria. Thus, *S. divaricata*, together with *S. arbusculiformis*, is the second intermediate to be identified in family Chenopodiaceae, a family that has been found to contain the most C_4 species among the dicots.

The carbon isotope composition of biomass is a means of analysing whether species are directly fixing atmospheric CO_2 via Rubisco or via PEPC in C_4 photosynthesis. In C_3 plants, Rubisco discriminates against fixing atmospheric $^{13}CO_2$ (resulting in more negative $\delta^{13}C$ isotope values), which is prevented or minimized in C_4 plants where atmospheric CO_2 is delivered to Rubisco in BS cells via the C_4 cycle. Previous studies showed that $\delta^{13}C$ values for C_4 plants are between −10‰ and −15‰. Typical $\delta^{13}C$ values for C_3 species are −24‰ to −30‰, but values in C_3 plants can become a few ‰ more positive (e.g. −21‰ to −22‰) in plants growing in arid conditions, where water stress can cause photosynthesis to be more limiting due to increased diffusive resistance (Cerling, 1999).

Analyses of the carbon isotope composition of the *Salsola* species in this study show that they have C_3-type values (average ranging from –22.6‰ in *S. montana* to –29.7‰ in *S. genistoides*) compared with the C_4-type values of *X. richteri* and *C. orientale* (–12.1‰ and –13.5‰, respectively). Analyses from gas exchange (including Γ), compartmentation of GDC between M and BS cells, and carbon isotope composition of biomass indicate that *S. masenderanica*, *S. montana*, *S. webbii*, and *S. genistoides* are functioning like C_3 species.

Salsola divaricata is a C_3–C_4 intermediate based on its reduced Γ, the selective localization of GDC in mitochondria of the KLCs, and other structural features. If intermediates fix atmospheric CO_2 via Rubisco with discrimination against fixation of $^{13}CO_2$ in M cells, and reduce Γ by refixing photorespired CO_2 in KLCs (Type I), their carbon isotope composition will be like that of C_3 plants; whereas, if they reduce photorespiration via a partially functioning C_4 cycle which does not discriminate against $^{13}CO_2$ (Type II), the isotope composition is expected to have an intermediate value (Edwards and Ku, 1987). The C_3-type isotope value of *S. divaricata* ($\delta^{13}C$ = –29.2‰) indicates that it is functioning as a type I intermediate. The low expression of C_4 cycle enzymes in this species is similar to that of the four C_3 species

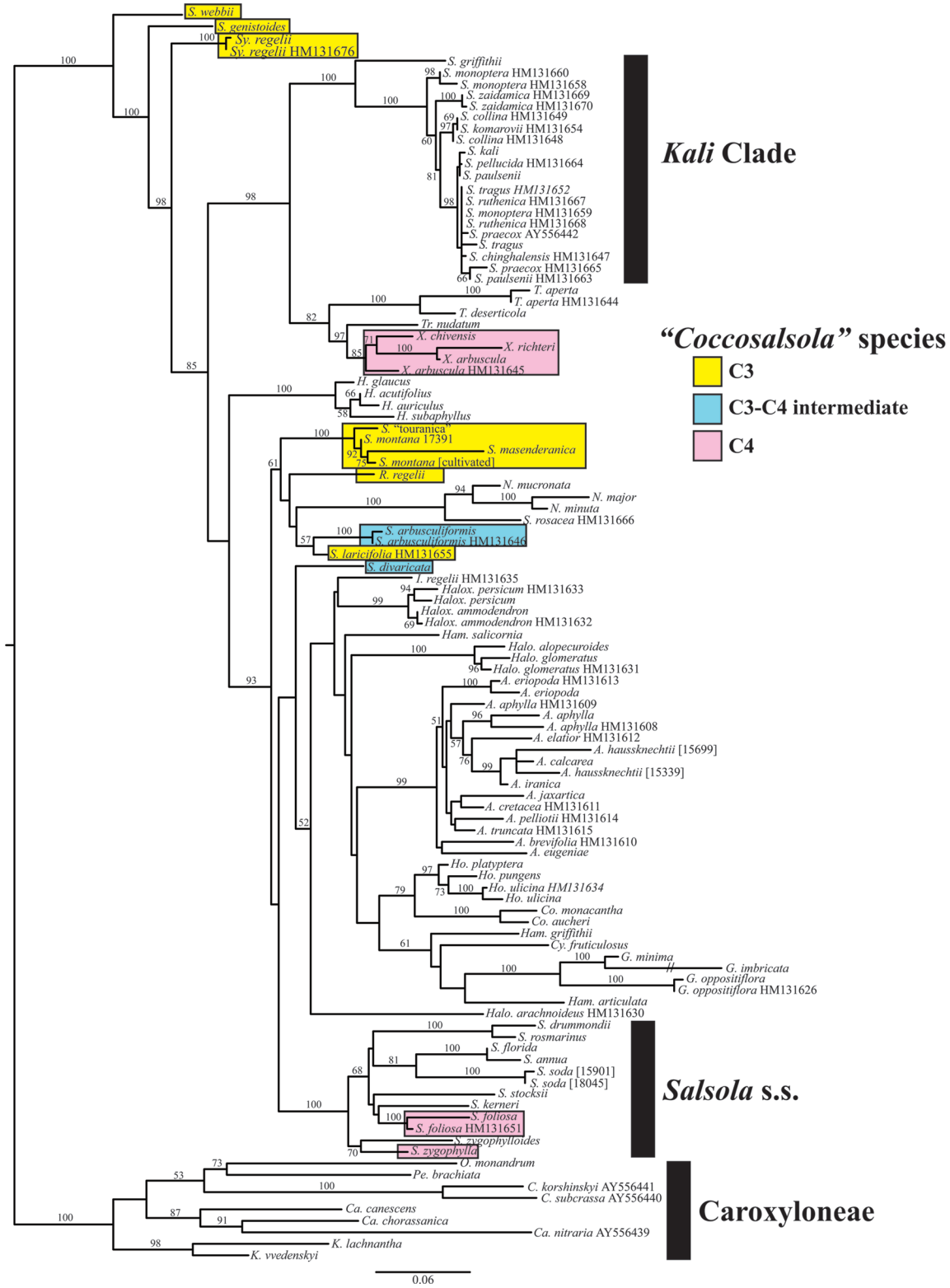

Fig. 8. Maximum likelihood phylogram of relationships in tribes Salsoleae and Caroxyloneae. Numbers at nodes reflect bootstrap percentages >50%. Genera are abbreviated as: *A.*, *Anabasis*; *C.*, *Climacoptera*; *Ca.*, *Caroxylon*; *Co.*, *Cornulaca*; *Cy.*, *Cyatobasis*; *G.*; *Girgensohnia*; *H.*; *Halothamnus*; *Halo.*, *Halogeton*; *Halox.*, *Haloxylon*; *Ham.*, *Hammada*; *Ho.*, *Horaninowia*; *I.*, *Iljinia*; *K.*, *Kaviria*; *N.*, *Noaea*; *O.*, *Ofaiston*; *Pe.*, *Petrosimonia*; *R.*, *Rhaphidophyton*; *S.*, *Salsola*; *Sy.*, *Sympegma*; *T.*, *Turania*; *Tr.*, *Traganum*; *X.*, *Xylosalsola*. The colour coding shows species from section '*Coccosalsola*' plus *S. touranica, Sy. regelii*, and *R. regelii*. The species boxed in blue are known C_3–C_4 intermediates in tribe Salsoleae. The species boxed in yellow have non-Kranz-type leaf anatomy and/or C_3-type carbon isotope composition (including *S. webbii*, *S. genistoides*, *S. montana,* and *S. masenderanica* in the present study; *S. laricifolia* putative intermediate based on structure but not functionally tested). The species boxed in pink are C_4 species from concept section *Coccosalsola*. The remaining species are C_4.

Table 6. *Summary of known types of photosynthesis in species of formerly* Salsola *section* Coccosalsola *(including* S. botschantzevii *and species added in Botchantzev, 1989)*

Informal genera	*Salsola* s.s.	*Xylosalsola* and not assigned
'Canarosalsola'		
S. divaricata C_3-C_4 (CI+A+P)	*S. cruciata* C_4 (CI)	*X. arbuscula* C_4 (CI+A+P)
'Collinosalsola'	*S. cyrenaica* C_4 (CI)	*X. chiwensis* C_4 (CI)
S. arbusculiformis C_3-C_4 (CI+A+P)	*S. drummondii* C_4 (CI+A)	*S. euryphylla*[a] C_4 (CI+A+P)
S. laricifolia C_3 (CI), C_3-C_4 (A)	*S. foliosa* C_4 (CI+A)	*X. paletzkiana* C_4 (CI+A+P)
'Oreosalsola'	*S. kerneri* C_4 (CI)	*X. richteri* C_4 (CI+A+P)
S. abrotanoides C_3 (CI)	*S. longifolia* C_4 (CI+A)	*S. transhyrcanica*[a] C_4 (CI)
S. botschantzevii C_3 (CI)	*S. makranica* C_4 (CI)	**Not assigned**
S. drobovii C_3 (CI), C_3–C_4 (A)	*S. melitensis* C_4 (CI)	*S. deschaseauxiana* C_3 (CI)
S. flexuosa C_3 (CI)	*S. oppositifolia* C_4 (CI+A)	*S. genistoides* C_3 (CI+A+P)
S. gymnomaschala C_3 (CI)	*S. schweinfurtii* C_4 (CI)	*S. webbii* C_3 (CI+A+P)
S. junatovii C_3 (CI)	*S. verticillata* C_4 (CI)	
S. lipschitzii C_3 (CI)	*S. zygophylla* C_4 (CI)	
S. masenderanica C_3 (CI+A+P)		
S. montana C_3 (CI+A+P)		
S. oreophila C_3 (CI+A+P)		
S. pachyphylla C_3 (A+CI)		
S. tianschanica C_3 (CI)		

A, anatomy; CI, carbon isotope composition; P, physiology.
[a] *Salsola euryphylla* Botsch. and *S. transhyrcanica* are presumed to belong to the *Xylosalsola* clade, but have not been included in any phylogenetic analyses and do not have a combination as of yet in *Xylosalsola*.

(*S. genistoides*, *S. masenderanica*, *S. montana*, and *S. webbii*, see Fig. 5) which suggests it has little or no capacity for C_4 function. In type I intermediates, any glycolate which is formed as a consequence of ribulose bisphosphate (RuBP) oxygenase activity in M cells will be metabolized in the glycolate pathway with generation of CO_2 via GDC in the KLCs. The Γ will be reduced to the extent photorespired CO_2 is refixed by the KLC chloroplasts. These intermediates have an advantage photosynthetically over C_3 species by refixation of photorespired CO_2 when CO_2 levels are limiting. Results from this study on carbon isotope composition in species of the formerly recognized section *Coccosalsola* show that 18 species have C_3-type $\delta^{13}C$ values (from –20.4‰ to –30.7 ‰). Two of these, *S. arbusculiformis* and *S. divaricata*, have now been shown to be C_3–C_4 intermediates.

Anatomical features

In subfamily Salsoloideae, most species are C_4 plants with Salsoloid-type Kranz anatomy, including the NAD-ME-type *C. orientale* and the NADP-ME-type *X. richteri* in this study (see the Introduction). In tribe Salsoleae, species lacking Kranz anatomy have previously been defined as having Sympegmoid-type leaf structure, with two well-developed layers of photosynthetic M cells and indistinctive BS cells having few chloroplasts. However, among the five *Salsola* species in the current study, along with the C_3–C_4 intermediate *S. arbusculiformis*, all of which have C_3-type carbon isotope composition, there are significant differences.

Three of these species (*S. genistoides*, *S. masenderanica*, and *S. webbii*), which functionally are C_3, have classical Sympegmoid-type anatomy with equally developed M1 and M2 photosynthetic cells, and indistinct BS cells. The BS cells have very few organelles, with chloroplasts and mitochondria distributed around the cells without any special positioning. *Salsola montana* also has Sympegmoid-type anatomy with quantitative features of M and BS cells similar to the above species. This includes M1 and M2 cells having equal lengths and widths (Fig. 2B, F; Supplementary Table S1 at *JXB* online; see also light micrograph in Akhani and Ghasemkhani, 2007). However, *S. montana* has greater development of organelles in BS cells, and the mitochondria are arranged along the inner or radial CW. This structural feature of BS cells occurs in all C_3–C_4 intermediates which have been studied. Thus, *S. montana* is classified as a proto-Kranz species, which is defined as a species exhibiting early development of a C_4 trait in BS cells, while functionally exhibiting C_3-type photosynthetic features. Proto-Kranz species have been found in a few genera in other families and they have been recognized as C_3 relatives in lineages having C_3–C_4 intermediate species (Muhaidat et al., 2011; Khoshravesh et al., 2012; Sage et al., 2012). In the BS cells of *S. montana*, some of the photorespired CO_2 from GDC, as a consequence of RuBP oxygenase activity in the BS chloroplasts, may be refixed (see discussion of proto-Kranz, Muhaidat et al., 2011). However, the effect on Γ would probably be small and very difficult to detect from gas exchange analysis, since the dual layers of M cells in *S. montana* account for most of the photosynthetic tissue (Fig. 2B, F; Supplementary Table S2), and dark-type respiration is also a component of Γ.

The C_3–C_4 intermediates *S. divaricata* (current study) and *S. arbusculiformis* (Voznesenskaya et al., 2001) have some features of Kranz-like anatomy. The cells of the outer M1 layer are much shorter and appear more like the hypodermal cells (if present) in C_4 Salsoloideae species. A similar

trend can be seen in leaf cross-sections of *S. laricifolia* (Wen and Zhang, 2011). Also, *S. drobovii* which has C_3 carbon isotope composition, represents another structural variant with a complete elimination of the outer M layer; it has only two layers of chlorenchyma characteristic of species with C_4 photosynthesis, M and KC (or KLC in this case; NKK and EVV, unpublished data). In *S. divaricata*, the layer of KLCs contains chloroplasts and numerous large mitochondria which are characteristic for other species with C_3–C_4 intermediate features (Edwards and Ku, 1987; Rawsthorne and Bauwe, 1998; Voznesenskaya et al., 2007, 2010; Muhaidat et al., 2011), including *S. arbusculiformis* (Voznesenskaya et al., 2001). The positioning of mitochondria in *S. divaricata* towards the inner CW is characteristic of all C_3–C_4 intermediates. Also, compared with the other four *Salsola* species in the current study, *S. divaricata* has some thickening of the CW of KLCs especially facing the intercellular space and adjacent to the WS tissue, a feature observed in Salsoloid anatomy, and a characteristic of many C_4 species which is considered to provide resistance to leakage of CO_2 from the KCs (von Caemmerer and Furbank, 2003).

In *S. divaricata*, the layer of KLCs is continuous around the leaf as in C_4 *Salsola* species. A similar arrangement of KLCs containing a visible layer of cytoplasm with organelles can also be seen in *S. laricifolia* (see fig. 13 in Wen and Zhang, 2011) and *S. drobovii* (EVV and NKK, unpublished), suggestive that they may functionally be a C_3–C_4 intermediate. In the other *Salsola* species in the current study (*S. genistoides*, *S. masenderanica*, and *S. webbii*), the BS cells adjacent to the small peripheral veins are represented by non-specialized parenchyma cells. In *S. masenderanica* and *S. montana*, they are similar to that observed previously for the C_3 species *S. oreophila* (Pyankov et al., 1997) and the C_3–C_4 intermediate *S. arbusculiformis* (Voznesenskaya et al., 2001), except for the difference in the number of organelles, with a higher number in *S. arbusculiformis* and *S. montana*, especially in the outermost BS cells occurring exactly above the vascular bundle.

From quantitative analysis, differences in the size and volume densities of tissues were identified between the M and BS cells of C_3 species (*S. genistoides*, *S. masenderanica*, *S. montana*, and *S. webbii*), the M cells and KLCs of the C_3–C_4 intermediates *S. arbuculiformis* and *S. divaricata*, and the M cells and KCs of representative C_4 species (Supplementray Table S1 at *JXB* online). The results show that the anatomy of the C_3–C_4 intermediate *S. arbuculiformis* is similar to that of the four C_3 *Salsola* species, with the exception that the intermediate has much smaller M1 cells, and more distinctive BS cells due to more numerous organelles. Both *S. arbusculiformis* and *S. divaricata* have smaller M1 cells and a larger investment in WS tissue than the C_3 species. The intermediate *S. divaricata* is unlike the C_3 species and the intermediate *S. arbusculiformis*, and rather like the C_4 species in having a lower volume density of M cells, a lower M/KLC ratio indicating an increased investment in KLCs, along with the Salsoloid-like anatomy.

Proposed sequence of evolution of Salsoloid-type C_4

C_4 species are considered to have evolved from C_3 ancestors. Based on the structural and functional differences between the *Salsola* species in this study, the previously identified C_3–C_4 intermediate *S. arbusculiformis*, and the C_4 species with Salsoloid-type anatomy, the following sequential structural and functional progression in evolution from C_3 to C_4 (or backward regression of C_4) is proposed (Fig. 9). Pre-conditioning for evolution of Salsoloid-type anatomy is increased succulence in C_3 species having Sympegmoid-type anatomy by adaptation to hot/dry climates and development of specialized WS tissue (Fig. 9A). In this study, the fraction of leaf tissue invested in WS tissue was lower in the C_3 species, with the lowest values in *S. genistoides* and *S. webbii* which are proposed to represent the ancestral condition for the other *Salsola* species.

C_3-type photosynthesis was shown by functional analyses for three *Salsola* species (*S. genistoides*, *S. masenderanica*, and *S. webbii*) which have Sympegmoid-type anatomy with two layers of photosynthetic tissue, M1 and M2, and with BS cells adjacent to veins having few organelles. For these three species, and especially for *S. genistoides* and *S. webbii*, the non-specialized BS cells, having only a few chloroplasts, contribute to the WS tissue rather than as chlorenchyma. The first proposed step towards development of Kranz anatomy is represented by the development of proto-Kranz features in *S. montana* (Fig. 9B). It has Sympegmoid-type anatomy; but, compared with the above species, it has an increase in the organelle number in BS cells and positioning of the mitochondria towards the inner BS CW. As in C_3 species, GDC is expressed equally in M and BS mitochondria, there is no thickening of the BS cell walls, and functionally it has C_3 traits. Also, the quantitative features of M and BS cells, and volume density of tissues in *S. montana* are similar to those of the other C_3 species.

The next steps in evolution involve establishment of the C_3–C_4 intermediate characters with Kranz-like anatomy (i.e. *S. arbusculiformis* and *S. divaricata*). This includes reduction of photosynthetic investment in M1 and an increased investment of development of KLCs. In the intermediates, the M1 cells appear more like the WS hypodermal layer found in some C_4 Salsoloid species, which suggests an evolutionary progression from M1 to hypoderm by reducing the cell length and organelle number. This could occur either by transforming the M1 cells to hypodermal cells, or by loss of the M1 layer (Salsoloid anatomy with and without a hypoderm, respectively). There is selective compartmentation of GDC to KLC mitochondria together with their enlargement, and the thickening of the KLC CWs which could decrease the loss of CO_2 from the KLC, and reduce Γ by refixing photorespired CO_2 in KLC.

The C_3–C_4 intermediate *S. arbusculiformis* has Kranz-like Sympegmoid anatomy with a discontinuous layer of KLCs which surround the separate vascular bundles. The anatomy is similar to that of the proto-Kranz species *S. montana* which has a large number of organelles in the BS cells. The main difference is that *S. arbusculiformis* has smaller M1 cells, and

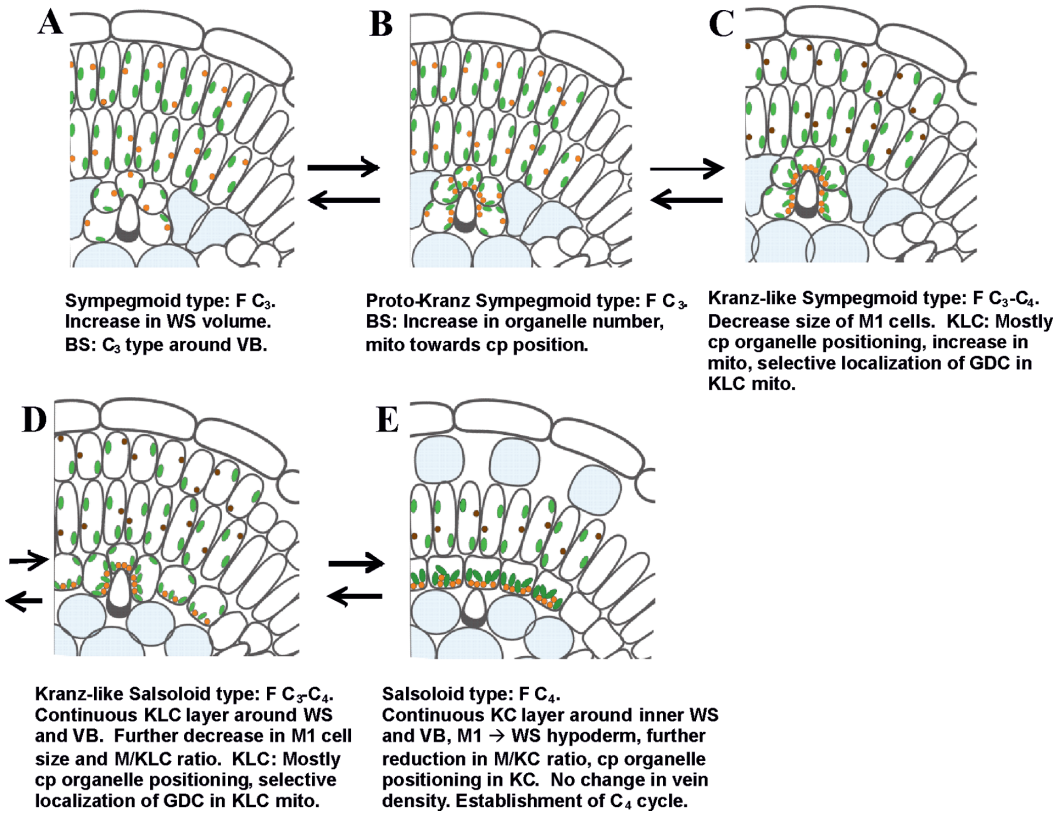

Fig. 9. A model illustrating five conceptual phases of evolution of C_4 Salsoloid-type anatomy, having a single compound Kranz unit, from C_3 Sympegmoid-type anatomy. Similar events might take place during reversions from C_4. Additional abbreviations: F, functional type; cp, centripetal, indicating positioning of organelles towards the inner BS, KLC, KC wall; mito, mitochondria. Colours: chloroplasts (green, dark green in KC in C_4), mitochondria (orange with GDC; dark brown without GDC).

the KLCs are specialized for selective decarboxylation of glycine in photorespiration (Fig. 9C). An important further step is development of a continuous layer of KLCs under the layer of M, as seen in the intermediate *S. divaricata* with Kranz-like Salsoloid anatomy (Fig. 9D). Having the structural development of Kranz anatomy with one layer of M chlorenchyma around the leaf periphery, with an underlying layer of small rounded KLCs, the final development of functional C_4 photosynthesis occurs by conversion of M1 to WS hypoderm and expression of the C_4 cycle between M and KCs, and selective expression of the C_3 cycle in the KC chloroplasts (Fig. 9E).

This proposed development of Salsoloid-type C_4 based on physiological and structural features of the species studied has in common some of the previously proposed biochemical modifications and steps in the progression from C_3 to C_4 photosynthesis (Edwards and Ku, 1987; Christin et al., 2011; Sage et al., 2012). In the model by Sage et al. (2012), which involves five phases, an important initial step is structural preconditioning of C_3 plants for closer positioning of veins and decreased numbers of M cells between veins as an adaptation to dry climates. Also, an important event is the enlargement of BS cells around the vascular tissue and reduction of the M/BS ratio. However, in this model, the structural changes were described for species having flat leaves and anatomy with so-called multiple simple Kranz units around individual veins according to the classification of Peter and Katinas (2003). C_4 Salsoloideae species have a single compound Kranz unit with all veins located inside the continuous double chlorenchyma layers. Analysis of patterns of venation in different types of *Salsola* species indicates that the type of photosynthesis and evolution to C_4 is not dependent on peripheral vein density; rather vein density is a species-specific character. Differences in vein density may reflect species-specific adaptations which depend on the environment and availability of water. Crucial events in the evolution of Salsoloid-type anatomy is a decrease in the layers of M cells and a significant increase in the number, but not the size of the KLCs or KCs. It is important to recognize that the current phylogenetic hypothesis (Fig. 8) does not suggest that the different stages described here represent a direct progression, in a phylogenetic sense, among the species described. Instead, it is suggested that the species described here represent different stages of progression in this model in parallel. One of the difficulties in the current study is that there is insufficient clarity in phylogenetic relationships, particularly in contrast to the patterns found in *Mollugo* (Christin et al., 2011), to test the number and precise direction of changes in the Salsoleae. While recognizing the basal position of C_3, *Sympegma*, *Salsola genistoides*, and *S. webbii*, species with intermediate features may represent either a progression in evolution of C_4 traits from C_3 ancestors or reversions from C_4.

In a treatment of representative *Salsola* species by Pyankov et al. (2001*b*), species lacking Kranz anatomy were distributed between two large branches within the tribe Salsoleae; one branch included mostly C_4 species with NAD-ME-type biochemistry and Salsoloid anatomy (together with several species having Sympegmoid-type anatomy, e.g. *S. oreophila*, *S. botschantzevii*, and *S. drobovii*), and another branch including NADP-ME-type species with Salsoloid anatomy (together with species lacking Kranz anatomy, e.g. *S. arbusculiformis* and *S. montana*). In a more detailed phylogeny, it was shown that the C_4 species with NAD-ME biochemistry belong to the tribe Caroxyloneae and the NADP-ME species belong to Salsoleae s.s. (Akhani et al., 2007). Furthermore, the results of that study show that section *Coccosalsola* is not monophyletic; C_4 species fall into two clades, the C_4 species of subsection *Coccosalsola* belong to the clade representing *Salsola* s.s. while the C_4 species of subsection *Arbusculae* were renamed to the genus *Xylosalsola* in tribe Salsoleae (*sensu* Akhani et al., 2007). Based on the analysis of one nuclear and one chloroplastic gene region (ITS and chloroplast *psbB-psbH*), sequences in phylogenetic schemes show that *S. masenderanica* and *S. montana* are very closely related species forming a clade with *S. arbusculiformis*, *Rhaphydophyton*, and *Noaea*, while *S. divaricata* forms an independent clade which is related to other C_4 species (Akhani et al., 2007). A close relationship between C_3 *S. montana* and *S. masenderanica*, the known C_3–C_4 intermediate *S. arbusculiformis*, and *S. laricifolia* is further supported by the maximum likelihood tree derived from ITS, *psbB-psbH*, and *rbc*L sequences (Wen et al., 2010). Similarly, a clade of *S. montana* and *S. masenderanica* is shown grouping with *S. arbusculiformis* (C_3–C_4 intermediate) and *S. laricifolia*, along with C_4 species of *Noaea* and *S. rosacea*. *Salsola laricifolia*, has a C_3-type isotope value (Table 5); Wen and Zhang (2011) suggested that this may be a C_3–C_4 intermediate based on it having a well-developed layer of KLCs. The C_3–C_4 species *S. divaricata* continues to be a lineage isolated from any of the other C_3 or C_3–C_4 intermediate species; however, better resolution and support will be necessary to clarify this.

Botschantzev (1976, 1985) considered *S. montana* Litv., *S. masenderanica* Botsch., *S. oreophila* Botsch., and *S. botschantzevii* Kurbanov to be separate species; later, Freitag and Rilke (1997) suggested that they all are synonyms for *S. montana* Litw. s.l.). However, ITS sequence data and anatomical differences given herein demonstrate at least the distinctness of *S. montana* and *S. masenderanica*. The distinctness of the other possible segregates of *S. montana* will require further study.

The evolutionary relationships of the Sympegmoid- and Salsoloid-type anatomies and gradations in between in tribe Salsoleae are still unclear. While a model for evolution from C_3 to C_4 developed from structural and physiological analysis has been proposed here, the model needs to be evaluated with a more robust phylogenetic hypothesis, which will require additional sequence data and species sampling. Earlier, Carolin et al. (1975) proposed that Sympegmoid anatomy evolved from Salsoloid, which is consistent with the suggestion of Pyankov et al. (1997, 2001*a*) that some C_3 Sympegmoid-type *Salsola* species, for example those occurring at higher elevations, may be reversions from C_4 species. However, Akhani et al. (1997) supported the idea that Salsoloid-type C_4 evolved from species having Sympegmoid-type anatomy; interestingly, *S. webbii*, *S. genistoides*, and *Sympegma regelii* form a grade leading to the rest of the Salsoleae (Fig. 8), which is consistent with this hypothesis. Similar positioning of *S. webbii* and *S. genistoides* has been previously suggested by Kadereit et al. (2003) and Kadereit and Freitag (2011), but with many fewer Salsoleae species sampled and with some variation in their precise position depending on the analysis. Here strong support is found for these species forming a grade at the base of the Salsoleae s.s. The phylogenetic patterns suggest that the ancestral species in Salsoleae are C_3 taxa such as *Sympegma regelii* (a Central Asian plant) and *Salsola genistoides* and *S. webbii* (two Iberian species). However, the C_3–C_4 intermediates and other C_3 species are all intertwined with C_4 clades (Fig. 8). It is therefore not clear whether there have been many origins of C_4 in this clade, or if in some cases these have been reversions from C_4. In the latter case, reversions from C_4 to intermediate to C_3 might occur by a gain of function of M cell chloroplasts to carry out C_3 photosynthesis by Rubisco, followed by a loss of this function in the KCs, accompanied by reversal of the structural features illustrated in Fig. 9. Further analysis will be necessary to determine the directions of change in photosynthetic pathways in this lineage. In the future, more detailed physiological and anatomical evaluations of all *Salsola* s.l. species with C_3 carbon isotope values are needed to determine whether they are C_3 or intermediates, along with phylogenetic analysis to consider how C_4 photosynthesis evolved in tribe Salsoleae.

Supplementary data

Supplementary data are available at *JXB* online.

Appendix S1. Sampling table for phylogenetic analysis.

Table S1. Mesophyll cell (M1, M2), hypodermal cell (H), bundle sheath cell (BS), Kranz-like cell (KLC), and Kranz cell (KC) sizes of *Salsola* s.l. species.

Table S2. Volume density of tissues (%) and ratios of M/BS in C_3, M/KLC in C_3–C_4, and M/KC in C_4 species of representative *Salsola* s.l.

Acknowledgements

This material is based upon work supported by the National Science Foundation grants IBN 0641232 and MCB 1146928, NSF Isotope Facility grant DBI-0116203, Civilian Research and Development Foundation grants RB1-2502-ST-03, RUB1-2829-ST-06, and RUB1-2982-ST-10, Russian Foundation of Basic Research grants 10-04-92512 and 12-04-00721, a grant for 'Geobotanical Studies in Different Parts of Iran IV' supported by the Research Council University of Tehran, and project no. 842951 supported by INSF. The field trip of H.A. to the Canary Islands was supported by Jardín Botánico Canario 'Viera y Clavijo' and the generous help of Dr Juli Caujapé-Castells. The authors are very grateful to Professor H. Freitag

for his valuable help including identification and providing material for carbon isotope composition analysis for some species, and advice in discussing relationships. We appreciate the material provided by herbariums (see Table 5), C. Cody for plant growth management, and the Franceschi Microscopy and Imaging Center of Washington State University for use of its facilities and staff assistance. EVV and NKK acknowledge the provision of equipment through the Core Center 'Cell and Molecular Technology in the Plant Science' at the Komarov Botanical Institute (St Petersburg).

References

Akhani H, Edwards G, Roalson EH. 2007. Diversification of the Old World Salsoleae s.l. (Chenopodiaceae): molecular phylogenetic analysis of nuclear and chloroplast data sets and a revised classification. *International Journal of Plant Sciences* **168,** 931–956.

Akhani H, Ghasemkhani M. 2007. Diversity of photosynthetic organs in Chenopodiaceae from Golestan National Park (NE Iran) based on carbon isotope composition and anatomy of leaves and cotyledons. *Nova Hedwigia* Suppl. **131,** 265–277.

Akhani H, Trimborn P, Ziegler H. 1997. Photosynthetic pathways in *Chenopodiaceae* from Africa, Asia and Europe with their ecological, phytogeographical and taxonomical importance. *Plant Systematics and Evolution* **206,** 187–221.

Bender MM, **Rouhani I**, **Vines HM**, **Black CC Jr**. 1973. $^{13}C/^{12}C$ ratio changes in Crassulacean acid metabolism plants. *Plant Physiology* **52,** 427–430.

Botschantzev VP. 1969. The genus *Salsola* L. (composition, history of development and distribution). Summary of report on published papers presented instead of doctor degree thesis. Leningrad: Nauka [In Russian].

Botschantzev VP. (in original publication cited as **Bochantsev**). 1976. Review of species of Coccosalsola Fenzl section of genus *Salsola* L. *Novosti Sistematiki Vysshikh Rastenii* **13,** 74–102 [In Russian].

Botschantzev VP. (in original publication cited as **Bochantsev**) 1985. *Review of species of the section Coccosalsola Fenzl, genus Salsola L.* (Translated from: *Novosti Sistematiki Vysshikh rastenii, vol. 13:74–102, 1976 = Obzor vidov sektsii Coccosalsola Fenzl roda Salsola L)*. Karachi: Muhammad Ali Society.

Botschantzev VP. 1989. De genere *Darniella* Maire et Weiller et relationes ejus ad genus *Salsola* L. (Chenopodiaceae). *Novosti Sistematiki Vysshikh Rastenii* **26,** 79–90 [In Russian].

Botschantzev VP, Kurbanov DK, Gudkova EP. 1983. Three new plant species from Turkmenia. *Botanicheskii Zhurnal* **68,** 236–238 [In Latin].

Butnik AA. 1984. The adaptation of anatomical structure of the family Chenopodiaceae Vent. species to arid conditions. Summary of biological science doctor degree thesis. Tashkent (In Russian): Academy of Sciences of UzbekSSR.

Carolin RC, Jacobs SWL, Vesk M. 1975. Leaf structure in Chenopodiaceae. *Botanische Jahrbücher für Systematik, Pflanzengeschichte und Pflanzengeographie* **95,** 226–255.

Castroviejo S, Luceño M. 1990. *Salsola* L. In: Castroviejo S, ed. *Flora Iberica* , vol. **2**. Madrid: El Real Jardín Botánico, CSIC, 542–547.

Cerling TE. 1999. Paleorecords of C_4 plants and ecosystems. In: Sage RF, Monson RK, eds. *C_4 plant biology* . New York: Academic Press, 445–469.

Christin P-A, Sage TA, Edwards EJ, Ogburn RM, Khoshravesh R, Sage RF. 2011. Complex evolutionary transitions and the significance of C_3–C_4 intermediate forms of photosynthesis in Molluginaceae. *Evolution* **65,** 643–660.

Delgado OR, Gallo AG, De La Torre WW. 2006. Nueva aportación al conocimiento de las comunidades rupícolas de la isla de Tenerife (islas Canarias): *Soncho congesti-Aeonietum holochrysi* ass. nova. *Vieraea* **34,** 7–16.

Edgar RC. 2004. MUSCLE: multiple sequence alignment with high accuracy and high throughput. *Nucleic Acids Research* **32,** 1792–1797.

Edwards GE, Ku MSB. 1987. The biochemistry of C_3–C_4 intermediates. In: Hatch MD, Boardman NK, eds. *The biochemistry of plants. Vol. 10. Photosynthesis*. New York: Academic Press, Inc., 275–325.

Edwards GE, Voznesenskaya EV. 2011. C_4 photosynthesis: Kranz forms and single-cell C_4 in terrestrial plants. In: Raghavendra AS, Sage RF eds. *C4 photosynthesis and related CO2 concentrating mechanisms*. Dordrecht, The Netherlands: Springer, 29–61.

Freitag H, Rilke S. 1997. *Salsola* L. (Chenopodiaceae). In: Rechinger KH, ed. *Flora Iranica. Flora des Iranischen Hochlandes und Umrahmenden Gebirge. Persien, Afghanistan, Teile von West-Pakistan, Nord-Iraq, Azerbaidjan, Turkmenistan*. Graz: Akademische Druck- und Verlagsanstalt, 154–255.

Fritzsch K, Brandes D. 1999. Flora und Vegetation salzbeeinflußter Habitate auf Fuerteventura. In: Brandes D, ed. *Vegetation salzbeeinflußter Habitate im Binnenland*. Braunschweig: Universitätsbibliothek der TU Braunschweig, 205–219.

Furbank R, von Caemmerer S, Sheehy J, Edwards G. 2009. C_4 rice: a challenge for plant phenomics. *Functional Plant Biology* **36,** 845–856.

Kadereit G, Borsch T, Weising K, Freitag H. 2003. Phylogeny of Amaranthaceae and Chenopodiaceae and the evolution of C_4 photosynthesis. *International Journal of Plant Sciences* **164,** 959–986.

Kadereit G, Freitag H. 2011. Molecular phylogeny of Camphorosmeae (Camphorosmoideae, Chenopodiaceae): implications for biogeography, evolution of C_4-photosynthesis and taxonomy. *Taxon* **60,** 51–78.

Khoshravesh R, Akhani H, Sage TL, Nordenstam B, Sage RF. 2012. Phylogeny and photosynthetic pathway distribution in *Anticharis* Endl. (Scrophulariaceae). *Journal of Experimental Botany* **65,** 5645–5658.

Long JJ, Berry JO. 1996. Tissue-specific and light-mediated expression of the C_4 photosynthetic NAD-dependent malic enzyme of amaranth mitochondria. *Plant Physiology* **112,** 473–482.

Maurino VG, Drincovich MF, Andreo CS. 1996. NADP-malic enzyme isoforms in maize leaves. *Biochemistry and Molecular Biology International* **38,** 239–250.

Muhaidat R, Sage TL, Frohlich MW, Dengler NG, Sage RF. 2011. Characterization of C_3–C_4 intermediate species in the genus *Heliotropium* L. (Boraginaceae): anatomy, ultrastructure and enzyme activity. *Plant, Cell and Environment* **34,** 1723–1736.

Peter G, Katinas L. 2003. A new type of Kranz anatomy in Asteraceae. *Australian Journal of Botany* **51,** 217–226.

Pyankov VI, Artyusheva EG, Edwards GE, Soltis PS. 2001*a*. Phylogenetic analysis of tribe Salsoleae of Chenopodiaceae based on ribosomal ITS sequences: implications for the evolution of photosynthetic types. *American Journal of Botany* **88,** 1189–1198.

Pyankov VI, Black CC Jr, Artyusheva EG, Voznesenskaya EV, Ku MSB, Edwards GE. 1999. Features of photosynthesis in *Haloxylon* species of Chenopodiaceae that are dominant plants in Central Asian deserts. *Plant and Cell Physiology* **40,** 125–134.

Pyankov V, Black C, Stichler W, Ziegler H. 2002. Photosynthesis in *Salsola* species (Chenopodiaceae) from Southern Africa relative to their C_4 syndrome origin and their African–Asian arid zone migration pathways. *Plant Biology* **4,** 62–69.

Pyankov VI, Vakhrusheva DV. 1989. Pathways of primary CO2 fixation in C-4 plants of the family Chenopodiaceae from the arid zone of Central Asia. *Soviet Plant Physiology* **36,** 178–187.

Pyankov VI, **Voznesenskaya EV**, **Kondratschuk AV**, **Black CC Jr**. 1997. A comparative anatomical and biochemical analysis in *Salsola* (Chenopodiaceae) species with and without a Kranz type leaf anatomy: a possible reversion of C_4 to C_3 photosynthesis. *American Journal of Botany* **84,** 597–606.

Pyankov VI, Voznesenskaya EV, Kuz'min AN, Ku MSB, Ganko E, Franceschi VR, Black CC Jr, Edwards GE. 2000. Occurrence of C_3 and C_4 photosynthesis in cotyledons and leaves of *Salsola* species (Chenopodiaceae). *Photosynthesis Research* **63,** 69–84.

Pyankov V, Ziegler H, Kuz'min A, Edwards GE. 2001*b*. Origin and evolution of C_4 photosynthesis in the tribe Salsoleae (Chenopodiaceae) based on anatomical and biochemical types in leaves and cotyledons. *Plant Systematics and Evolution* **230,** 43–74.

Rawsthorne S, Bauwe H. 1998. C_3–C_4 intermediate photosynthesis. In: Raghavendra AS, ed. *Photosynthesis. A comprehensive treatise* . Cambridge: Cambridge University Press, 150–162.

Rawsthorne S, Hylton CM, Smith AM, Woolhouse HW. 1988. Photorespiratory metabolism and immunogold localization of photorespiratory enzymes in leaves of C_3 and C_3–C_4 intermediate species of *Moricandia*. *Planta* **173,** 298–308.

Sage RF, Christin P-A, Edwards EJ. 2011. The C_4 plant lineages of planet Earth. *Journal of Experimental Botany* **62,** 3155–3169.

Sage RF, Sage TL, Kocacinar F. 2012. Photorespiration and the evolution of C_4 photosynthesis. *Annual Review of Plant Biology* **63,** 19–47.

Stamatakis A, Hoover P, Rougemont J. 2008. A rapid bootstrap algorithm for the RAxML web-servers. *Systematic Biology* **75,** 758–771.

von Caemmerer S, Furbank RT. 2003. The C_4 pathway: an efficient CO_2 pump. *Photosynthesis Research* **77,** 191–207.

Voznesenskaya EV. 1976. Ultrastructure of assimilating organs of some species of the family Chenopodiaceae. II. *Botanicheskii Zhurnal* **61,** 1546–1557 [In Russian].

Voznesenskaya EV, Akhani H, Koteyeva NK, Chuong SDX, Roalson EH, Kiirats O, Franceschi VR, Edwards GE. 2008. Structural, biochemical and physiological characterization of photosynthesis in two C_4 subspecies of *Tecticornia indica* and the C_3 species *Tecticornia pergranulata* (Chenopodiaceae). *Journal of Experimental Botany* **59,** 1715–1734.

Voznesenskaya EV, Artyusheva EG, Franceschi VR, Pyankov VI, Kiirats O, Ku MSB, Edwards GE. 2001. *Salsola arbusculiformis*, a C_3–C_4 intermediate in Salsoleae (Chenopodiaceae). *Annals of Botany* **88,** 337–348.

Voznesenskaya EV, Gamaley YV. 1986. The ultrastructural characteristics of leaf types with Kranz-anatomy. *Botanicheskii Zhurnal* **71,** 1291–1307 [In Russian].

Voznesenskaya E, Koteyeva NK, Chuong SDX, Ivanova AN, Barroca J, Craven L, Edwards GE. 2007. Physiological, anatomical and biochemical characterization of the type of photosynthesis in *Cleome* species (Cleomaceae). *Functional Plant Biology* **34,** 247–267.

Voznesenskaya EV, Koteyeva NK, Edwards GE, Ocampo G. 2010. Revealing diversity in structural and biochemical forms of C_4 photosynthesis and a C_3–C_4 intermediate in genus *Portulaca* L. (Portulacaceae). *Journal of Experimental Botany* **61,** 3647–3662.

Wen Z-B, Sanderson SC, Zhu G-L, Zhang M-L. 2010. Phylogeny of Salsoleae s.l. (Chenopodiaceae) based on DNA sequence data from ITS, *psb*B-*psb*H, and *rbc*L, with emphasis on taxa of northwestern China. *Plant Systematics and Evolution* **288,** 25–42.

Wen Z, Zhang M. 2011. Anatomical types of leaves and assimilating shoots and carbon 13C/12C isotope fractionation in Chinese representatives of Salsoleae s.l. (Chenopodiaceae). *Flora – Morphology, Distribution, Functional Ecology of Plants* **206,** 720–730.

Winter K. 1981. C_4 plants of high biomass in arid regions of Asia. Occurrence of C_4 photosynthesis in Chenopodiaceae and Polygonaceae from the middle east and USSR. *Oecologia* **48,** 100–106.

Woodrow IE, Berry JA. 1988. Enzymatic regulation of photosynthetic CO_2 fixation in C_3 plants. *Annual Review of Plant Physiology and Plant Molecular Biology* **39,** 533–594.

Zalenskii OV, Glagoleva T. 1981. Pathway of carbon metabolism in halophytic desert species from Chenopodiaceae. *Photosynthetica* **15,** 244–255.